




Review

# Role of Tunable Gold Nanostructures in Cancer Nanotheranostics: Implications on Synthesis, Toxicity, Clinical Applications and Their Associated Opportunities and Challenges

Akash Kumar <sup>1,2</sup>, Nabojit Das <sup>1,2,\*</sup> and Raja Gopal Rayavarapu <sup>1,2,\*</sup> 

<sup>1</sup> Nanomaterial Toxicology Laboratory, Systems Toxicology and Health Risk Assessment Group, CSIR-Indian Institute of Toxicology Research (CSIR-IITR), Vishvgyan Bhawan, 31 Mahatma Gandhi Marg, Lucknow 226001, India

<sup>2</sup> Academy of Scientific and Innovative Research (AcSIR), Ghaziabad 201002, India

\* Correspondence: rajagopal@iitr.res.in

**Abstract:** The existing diagnosis and treatment modalities have major limitations related to their precision and capability to understand several stages of disease development. A superior therapeutic system consists of a multifunctional approach in early diagnosis of the disease with a simultaneous progressive cure, using a precise medical approach towards complex treatment. These challenges can be addressed via nanotheranostics and explore suitable approaches to improve health care. Nanotechnology in combination with theranostics as an unconventional platform paved the way for developing novel strategies and modalities leading to diagnosis and therapy for complex disease conditions, ranging from acute to chronic levels. Among the metal nanoparticles, gold nanoparticles are being widely used for theranostics due to their inherent non-toxic nature and plasmonic properties. The unique optical and chemical properties of plasmonic metal nanoparticles along with theranostics have led to a promising era of plausible early detection of disease conditions, and they enable real-time monitoring with enhanced non-invasive or minimally invasive imaging of several ailments. This review aims to highlight the improvement and advancement brought to nanotheranostics by gold nanoparticles in the past decade. The clinical use of the metal nanoparticles in nanotheranostics is explained, along with the future perspectives on addressing the key applications related to diagnostics and therapeutics, respectively. The scope of gold nanoparticles and their realistic potential to design a sophisticated theranostic system is discussed in detail, along with their implications in clinical advancements which are the needs of the hour. The review concluded with the challenges, opportunities, and implications on translational potential of using gold nanoparticles in nanotheranostics.

**Keywords:** anisotropy; gold nanostructures; nanotheranostics; plasmonic; toxicity



**Citation:** Kumar, A.; Das, N.; Rayavarapu, R.G. Role of Tunable Gold Nanostructures in Cancer Nanotheranostics: Implications on Synthesis, Toxicity, Clinical Applications and Their Associated Opportunities and Challenges. *J. Nanotheranostics* **2023**, *4*, 1–34. <https://doi.org/10.3390/jnt4010001>

Academic Editors: Ajeet Kaushik, Isha Mutreja and Dhiraj Kumar

Received: 16 November 2022

Revised: 21 December 2022

Accepted: 26 December 2022

Published: 6 January 2023



**Copyright:** © 2023 by the authors. Licensee MDPI, Basel, Switzerland. This article is an open access article distributed under the terms and conditions of the Creative Commons Attribution (CC BY) license (<https://creativecommons.org/licenses/by/4.0/>).

## 1. Introduction

### 1.1. Cancer Theranostics: Early Strategies

Cancer is one of the most complex diseases causing millions of deaths every year, against which early detection and treatment require concerted efforts [1]. The existing modalities and approaches are limited to diagnosis and treatments which include chemotherapy, radiation, appropriate surgery, and the use of anti-cancer drugs [2,3]. The availability of adequate resources and advanced technology are not enough to provide proper management of the disease due to certain limitations. The unavailability of an appropriate diagnostic system, among other reasons such as uncertainty of the target, low enhanced permeability and retention effect (EPR), and the lack of an appropriate drug delivery system, and multidrug resistance are the contributing factors [4]. The most prominent roadblock to effective cancer treatment is an early-stage diagnosis. Therefore, in order

to enable full-fledged cancer treatment, a novel material or technology is the demand of the hour. The developed material or technology must align with demands such as target specificity and selectivity. Furthermore, the safe design of the material is critical in keeping view of the requirement for reduced biodistribution, and a distant reach of the target. The system or the material developed should be advanced enough—where simultaneous diagnosis and treatment is possible. The simultaneous diagnosis and treatment of a disease condition is called a theranostic approach, which reduces the delay in curing the disease [5]. Currently, theranostic based treatment is being effectively used in neurodegenerative diseases, rheumatoid arthritis, cardiovascular diseases, and bacterial infections [6–10]. Cancer theranostics concomitantly include the identification of new biomarkers for molecular diagnosis: molecular imaging probes; techniques for early detection; molecular imaging-based cancer therapy; nanoplateforms-assisted materials for advanced drug delivery and treatment. Cancer biomarkers significantly indicate the development of cancer through their up-down regulation due to abnormal cellular activity in cancerous cells. Biomarker assessment is the first step in identifying changes in normal metabolic processes, which can be easily evaluated using advanced approaches such as metabolomics, proteomics, genome sequencing, and computational analysis [11]. The information obtained from the biomarker assessment can be used for prescribing personalized medicine based on the level of damage.

In most cases, in vivo imaging methods are preferred following biomarker analysis. The techniques are non-invasive and include magnetic resonance imaging (MRI), positron emission tomography (PET), single-photon emission computed tomography (SPECT), ultrasound imaging (USI), photoacoustic imaging (PAI), and optical imaging (OI). These techniques have their limitations and strengths. For instance, USI is a low-cost technology with higher resolution but lower contrast. MRI has a high penetration capacity and image resolution but has low sensitivity, sluggish imaging speed, and is expensive. PET has excellent sensitivity but low spatial resolution and inadequate ionizing radiation [12]. A similar approach, called image-guided therapy has also been used for the treatment of cancer, either invasively or non-invasively depending on the condition of the lesion. Radiofrequency ablation (tumor destruction by radio waves), microwave ablation (tumor destruction by microwave), cryoablation (by freezing), and chemoembolization (lesion destruction by chemicals) are used simultaneously during image-guided therapy [13]. The existing treatment strategies have limitations which limit the efficient treatment of cancer, leading to recurrence of the disease. However, the recent advances in the theranostic applications using nanotechnology have shown a silver lining in fighting cancer. The early diagnosis led to the proper management of the disease. The term “nanotheranostics” is used specifically for theranostic application involving materials in the nano regime. These nanomaterials/nanoparticles are utilized in simultaneous detection and therapy with high effectiveness and fewer side effects.

### *1.2. Importance and Properties of Gold Nanostructures*

The use of gold in modern medicine flourished from the late 19th century to the early 20th century, during which the treatment regimens showed considerable advancement [14]. Since then, noble metal nanoparticles have received considerable attention in several biological applications such as drug delivery, therapy, imaging, and antimicrobial related applications [15]. Among the noble metals, gold is the most frequently used metal for the synthesis of nanoparticles due to ease of synthesis, surface modification, and superior optical and thermal properties [16]. The properties of gold nanoparticles are highly dependent on their size, shape, and surface chemistry and can be modulated accordingly.

The size and shape of gold nanoparticles are also influenced by synthetic processes such as photochemical, laser ablation, ball milling, sonochemical, wet chemical reduction, and green synthesis [17]. Among the several methods, the wet chemical reduction method has been widely appreciated for developing materials intended for biomedical applications, due to excellent monodispersity and high yield of the product formed. Spherical gold

nanoparticles (AuNPs) are the most commonly synthesized materials for targeted drug delivery and efficient drug loading. Gold nanospheres of different sizes are traditionally synthesized by reducing  $\text{HAuCl}_4$  (gold salt) with various reducing agents at different temperatures and pressures. Trisodium citrate is a commonly used reducing and stabilizing agent capable of synthesizing monodispersed gold nanospheres of different particle sizes by varying the concentration of citrate [18]. In order to synthesize large particles (>50 nm) devoid of irregular shapes, the seed-mediated approach is used in which a pre-formed seed (<5 nm) is added in the presence of reducing agents such as ascorbic acid, 2-mercaptosuccinic acid, hydroquinone, and hydrogen peroxide [19–22]. Nevertheless, the use of gold nanospheres is limited in theranostic applications due to their confined absorbance in the visible region. The therapeutic potential of chemically synthesized gold nanoparticles in photothermal therapy, imaging, and biosensing has been recognized for the ability to exhibit absorbance in the near infra-red/infra-red (NIR-IR) region [23–25]. Anisotropic nanoparticles, particularly nanorods, have been used more frequently, as compared to other shapes for NIR-IR-based diagnosis and simulation-based drug delivery in cancer therapy [26]. The gold nanorods with high monodispersity were synthesized using a template-directed seed-mediated approach. In the seed-mediated approach, gold seeds are prepared using a strong reducing agent in the presence of cetyl trimethyl ammonium bromide (CTAB) [27]. Prepared seed was added to the reaction mixture known as growth solution, which contains gold salt, silver nitrate, ascorbic acid, and CTAB. The aspect ratio of gold nanorods can be controlled by modulating the reaction parameters, such as the concentration of silver nitrate and the amount of seed [28,29]. Apart from gold nanorods, gold nanoshells are typically made of dielectric core materials (such as silica and polystyrene) that are coated with a thin gold layer. Core materials such as silica and polystyrene are widely used to provide high stability and monodispersity [30]. The dimensions of the core and/or the shell of these core materials can be tailored; typically, the core has a diameter of 100 nm and a thin gold shell of several nanometers (1–20 nm) [31,32]. A common method for preparing gold nanoshells is to modify the core surface with a bifunctional ligand that improves shell coverage. The core surface of silica is modified by 3-aminopropyltriethoxysilane (APS) which contains both ethoxy and amine groups. The ethoxy group binds covalently to the silica surface through the hydroxyl group, whereas the amine group binds to the gold shell surface. Furthermore, bifunctional linkers such as 3-aminopropyltrimethoxysilane (APTMS) and 3-mercaptopropyltrimethoxysilane (MPTMS) are used to modify the silica, resulting in amino- and thiol-functionalized surfaces that can efficiently bind to the gold surface. As a result of aging, the gold binds to the silica core forming the entire shell [33]. However, gold nanocages, that are hollow in nature with controlled pore size on the surface, are synthesized by the galvanic replacement reaction between truncated silver (Ag) nanocubes and gold chloride ( $\text{HAuCl}_4$ ) [34]. Silver nanostructures with controlled shapes can be synthesized using the polyol reduction method in which  $\text{AgNO}_3$  is reduced by ethylene glycol to produce Ag atoms, and followed by the formation of nanocrystals or seeds. Silver nanostructures are used as a precursor and can be galvanically replaced to form gold nanoparticles with hollow structures. The dimensions and thickness of the wall in gold nanocages were controlled by adjusting the molar ratio of Ag to  $\text{HAuCl}_4$  [34]. However, in the case of synthesizing gold nanoparticles of various shapes, several cappings are used which also provides colloidal stability. In chemical synthesis, sodium borohydride or sodium hydride, sodium citrate, or ascorbic acid act as capping and stabilizing agents for the gold nanoparticles. However, in green synthesis, extracts from plants are used to synthesize nanoparticles. A wide range of reactive compounds found in biomass also participate in the synthesis and stabilization processes. Several studies have reported the green synthesis of highly stable AuNPs [35–37]. Furthermore, altering the concentration of gold salt used in the synthesis reaction, as well as the pH and temperature, provides control over the size and shape of gold nanoparticles. The Derjaguin Landau Verwey Overbeek theory (DLVO) described the entire process of metallic nanoparticle stabilization [38,39]. Therefore, nanoparticle stabilization with different cappings such as

polymers, surfactants, biomolecules, and proteins is necessary for ensuring the integrity of the nanoparticles' physicochemical properties [40–42].

Gold nanoparticles have generated significant interest owing to their exceptional plasmonic properties. The external laser (incident light) excites a collective and coherent oscillation of conduction electrons near the surface of the gold nanoparticle, and this oscillates with the frequency of incident light, resulting in scattering and spectral absorption called localized surface plasmon resonance (LSPR) [43,44].

Gold nanoparticles exhibit LSPR over a wavelength range of electromagnetic radiation, from Vis to the near-infrared/infrared (NIR/IR) region that is tunable through size-shape modulation of nanoparticles during synthesis [45]. For example, gold nanorods (AuNRs) with greater aspect ratios exhibit a significant red shift in the near-infrared region [46]. Unlike AuNRs, gold nanoshells are highly sensitive to shell thickness, resulting in modulation of their plasmonic properties [47]. The LSPR of AuNPs is highly dependent on the interaction between gold nanoparticles and the supporting substrate due to changes in the refractive index of the surrounding medium. When the local refractive index of the nanoparticles increases, the LSPR frequency decreases and vice versa [48]. In addition, LSPR is used in many techniques but however ultrasmall gold nanoparticles—so called gold nanoclusters (<3 nm)—do not show any LSPR compared to the large gold nanosphere. These nanoclusters exhibit intrinsic fluorescence at the wavelengths ranging from the visible to the NIR region, upon excitation at the UV region. Gold nanoclusters have become an interesting sensing and imaging material due to their long half-life, large stokes shift, and biocompatibility [49–52]. The free-electron theory is especially important for understanding the fundamental optical properties of gold nanoclusters which work quite well in most cases. The free electron on the surface of nanoparticles creates polarization where the number of electrons determine the size-dependent plasmonic optical properties [53]. However, a decrease in the number of free electrons below a critical value lead toward continuous band splits into discrete energy levels as the nanoparticle size reaches the Fermi wavelength [54]. The numeric size of the energy level spacing determines the fluorescence of gold nanoclusters. This intrinsic fluorescence of gold nanoclusters is utilized for imaging and therapy in cancer theranostics.

Gold nanoparticles showed promising potential in nanomedicine, drug delivery, targeting, and bioimaging due to their diverse functionalities. Additionally, the inherent non-toxic nature of gold established its candidature in theranostic applications. This was confirmed through several studies where gold nanostructures showed a non-toxic nature with a higher degree of biocompatibility. Our previous study confirmed the size independent non-cytotoxic nature of gold nanospheres capped with taurine (a non-protein amino acid) in HepG2 cells [55]. In another study, gold nanoparticles (20 nm) were prepared using green fungus (*Ganoderma* sp.) extract, which showed no cytotoxicity in breast cancer cells (MDA-MB-231). In addition, the synthesized nanoparticles showed high monodispersity and enhanced biocompatibility [56]. These advantages of the gold nanostructures make them an ideal candidate in cancer theranostics.

### 1.3. Role of Tunable Gold Nanostructures in Cancer Theranostics

Nanomaterials used for cancer theranostics aid non-invasive, real-time monitoring and treatment by killing cancerous cells without affecting normal healthy cells in the vicinity [57,58]. While using a nanotheranostic approach, the physician can tailor the patient's treatment regime according to the disease state and response; thereby, they can avoid unwanted side effects, multiple drug resistance, complete remission, and relapse [59,60]. Nanocarriers in theranostic applications easily enter cancer cells which have leaky blood vessels and lymphatic system, resulting in rapid uptake of the therapeutic agent. This results in gradual nanoparticle accumulation at the tumor site, with improved permeability and retention effect (EPR) [61]. The EPR effect enhances the efficiency of nanoparticles due to higher retention time, which is not observed while using drugs only. Gold nanoparticles are commonly used after functionalization with various molecules such as antibodies or



drugs depending upon the intended application. However, without drugs or conjugated moieties, gold nanoparticles of anisotropic shapes exhibit NIR-IR absorption, killing cancer cells through a heat-induced mechanism called plasmonic photothermal therapy [62].

The mechanism of photothermal therapy involves the induction of local hyperthermia in cancer cells. Hyperthermia occurs due to the increase in temperature (42–45 °C) upon NIR laser irradiation at the local site, leading to intrinsic or extrinsic ER (endoplasmic reticulum)-mediated apoptosis [63]. Yujuan Zhang et al. (2018) reported a temperature-dependent cell death pattern upon using gold nanoparticles for phototherapy-mediated cancer therapy. The study concluded apoptosis-mediated cell death at a temperature below 50 °C and not exceeding it, while an elevated temperature above 50 °C triggered necrosis-mediated cell death [64]. The role of a nanostructure-based platform in theranostics includes nanoformulation tracking, drug delivery kinetics, targeted drug delivery with concurrent diagnosis, thus assisting strategy evaluation and efficiency optimization. Despite being at a nascent stage, the advent of nanotheranostics that uses nanoparticle-mediated approach to cancer diagnosis and treatment has shown a considerable amount of promising potential [65].

This review article elaborately discussed the role of gold nanostructures in cancer diagnosis and therapeutic application using theranostic based approaches. The designing strategies of gold nanoparticles for cancer theranostics are based on their physicochemical properties: size, shape, surface modification, and conjugation which has been discussed in detail (Figure 1). The potential toxic effects of gold nanostructures are highlighted using in vitro and in vivo model systems for their limited use in cancer theranostics. Several applications of gold nanoparticles have also been discussed, including targeted drug delivery, therapeutic drugs, phototherapy, and bioimaging. The review concluded with a discussion on clinical/preclinical strategies and challenges associated with using gold nanostructures in cancer theranostics.

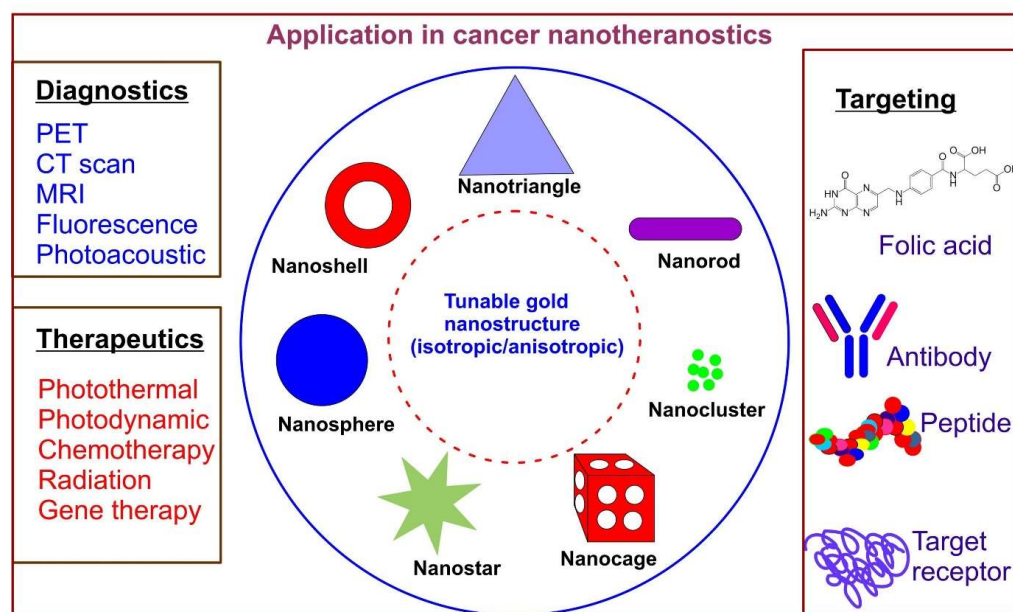


**Figure 1.** The schematic illustrating the shape by design of tunable gold nanostructures from isotropy to anisotropy through surface modification and their application in cancer nanotheranostics.

## 2. Designing Strategies of Gold Nanostructures for Cancer Theranostics

### 2.1. Tuning the Size and Shape Design of Gold Nanostructures

Gold nanoparticles are well known for their superior physicochemical properties such as surface plasmon resonance (SPR), high photothermal conversion rate, easy synthesis of various shapes and sizes, and high water stability, which provides a platform for easy surface functionalization with various functional molecules [16,62]. Functionalization of nanoparticles is critical because it provides target specificity along with bioavailability enhancement of the functional molecule, which is generally a drug or a signaling molecule used for therapeutic purposes and diagnosis, respectively. The gold nanoparticle's size and shape are tuned accordingly for imaging and phototherapy i.e., photodynamic therapy and photothermal therapy (PDT/PTT), respectively. It also influences stimulus-dependent drug delivery leading towards advancement of the treatment regime.

Gold nanoparticles can be classified into isotropic and anisotropic nanostructures based on their morphology [66]. Anisotropic shapes include every shape other than spherical, which renders them as having unique physico-chemical properties compared to the latter. The advantages of anisotropic nanostructures is mainly due to their ability to absorb light in the NIR-IR region which is not observed in isotropic nanoparticles (except hollow nanospheres). This unique feature of gold nanoparticles enables them to be used for photothermal therapy (PTT) or photodynamic therapy (PDT) during cancer treatment.

#### 2.1.1. Isotropic Gold Nanostructures

Metal–gold nanoparticles and their applications: as a biosensor, imaging agent, therapeutic molecule, and nano-vehicle for targeted drug delivery, are highly dependent on their structural properties [67]. Various end-user applications of gold nanostructures have been achieved by modulating the structural properties of nanoparticles using different synthetic procedures. Spherical nanoparticles are the most commonly synthesized nanoparticles due to their ease of synthesis and surface modification. Furthermore, well-developed synthetic methods were employed for synthesizing size-tunable and highly monodispersed spherical nanoparticles [68]. In clinical bio-nanomedicine, monodispersed gold nanoparticles are advantageous due to a high amount of drug loading onto the nanoparticle's surface making them efficient in drug delivery and therapeutic efficacy, respectively. Gold nanospheres stabilized with polyethylene glycol (PEG) and polyethyleneimine (PEI) exhibited robust stability in the biological environment [69]. The specificity achieved in diagnosing cancer through imaging involved receptor–ligand conjugation of the nanoparticles. These conjugated nanoparticles bind to the receptors (biomarkers) that are overexpressed in cancer cells due to abnormal metabolism. For instance, a commonly overexpressed biomarker in cancer cells is the folic acid receptor which allows for selective targeting by conjugating a folic acid ligand to the nanoparticles [70]. A similar approach, through alteration of target selectivity and specificity towards the targeting receptor can be adopted for diagnosis. For example, gold nanospheres labelled with fluorescent tags or dye are used as nanoprobe for imaging purposes [71].

Apart from specific targeting, functional entities conjugated to nanoparticles play a major role in deciphering the drug delivery mechanism through target accumulation. Similarly, it was reported that PEGylated gold nanospheres conjugated with T cells were used to monitor T cell kinetics and their biodistribution through imaging [72]. The evaluation of target site damage, drug distribution, drug release kinetics, and drug administration for therapeutic purposes was possible due to strategies used in nanotheranostics. Several published reports in the literature are compiled (as shown in Table 1) based on the potential use of isotropic gold nanostructures as a theranostic nanoprobe for detection/imaging or targeting tumors [73–86]. These reports show that gold nanoparticles have a tremendous capability in enabling theranostic-based nanomedicine.

**Table 1.** Compilation of several reported studies on using isotropic gold nanoparticles in cancer nanotheranostics and their respective in vitro/in vivo safety assessment.

Gold Nanoparticles (Size/ Shape)	Model System	Targeted Cancer	Therapy	Imaging/Modalities	Reference
Gold nanospheres (60 nm)	Zebrafish	Prostate cancer	Plasmonic nanobubble (PNB)	Scattering	[73]
Gold nanobeacons	MGC-803, tumor bearing mice	Gastric cancer	Gene silencing	Fluorescence	[74]
Gold nanobeacons	MDA-MB-231, tumor-bearing mice	Breast cancer	Chemotherapy	Fluorescence	[75]
Gold nanospheres (15 nm)	A549 cells, Balb/c mice	Lung cancer	Gene silencing	Fluorescence	[76]
Gold nanospheres (14 nm)	MCF-7, BALB/c nude mice	Breast cancer	PTT	CT, PTT imaging	[77]
Gold nanospheres (5 nm)	9L.E29 cells and athymic mice	Brain cancer	PDT	Fluorescence	[78]
Gold nanospheres (60 nm)	HN31 cell line, J32 cells and HNSCC model mouse	Cells overexpressed EGFR	PNB	Photoacoustic imaging	[79]
Gold nanospheres (90 nm)	HT-adenocarcinoma cells, B6 albino mice	Cells overexpressed EGFR	Chemotherapy (Raman-drug)	SERS	[80]
Gold nanospheres (33 nm)	CK, 4T1-GFP, and 2H11 cells, A/J mice	Lung cancer	PTT	Photoacoustic imaging	[81]
Hollow gold nanospheres (40–50 nm)	HeLa cells, Nude mice	Cervical cancer	Gene silencing	PET	[82]
Gold nanoclusters (1 nm)	A549, HTC116, MDA-MB-231, HepG2 cells and S180-tumor bearing mice model	Lung, liver, breast, colon cancers	Chemotherapy	Fluorescence	[83]
Gold nanoparticles (4 nm, 2 nm)	A431 cells	Squamous cell carcinoma	PTT	Photoacoustic imaging	[84]
Hollow gold nanospheres (37 nm)	A2780, A549 cells and Swiss mice	EphB4 expressing tumor cell	PTT	SPECT	[85]
Iron Oxide-gold nanospheres (6–18 nm)	SW1222,	Colorectal cancer	PTT	MRI	[86]

Note: PTT, Photothermal Therapy; PDT, Photodynamic Therapy; CT, Computed Tomography; MRI, Magnetic Resonance Imaging; PET, Positron Emission Tomography; SPECT, Single-Photon Emission Computed Tomography; PNB, Plasmonic Nanobubble; SERS, Surface Enhanced Raman spectroscopy.

### 2.1.2. Anisotropic Gold Structures

The anisotropic gold nanoparticles were reported in the early 20th century (1917) by Zsigmondy. For his contribution to the field of colloidal chemistry, Zsigmondy received the Nobel prize in chemistry (1925) [87]. The hexagonal and pentagonal-shaped gold nanoparticles were synthesized in 1979 and 1981 using the chemical vapor deposition method [88,89]. The widely explored anisotropic-shaped nanoparticles, i.e., rod-shaped, were synthesized by Wiesner and Wokaun in 1989 using the wet chemical reduction method [90]. In 1912,

Gans extended the concept of Mie's theory to anisotropic nanoparticles absorbing light in a more extended wavelength range, as compared to spherical nanoparticles [91]. In particular, anisotropic gold nanoparticles (including hollow gold nanospheres) exhibit an absorption spectrum in the NIR region. The NIR transition in 600–1300 nm opens the window for non-invasive optical imaging, photothermal therapy, and imaging modalities [92]. Anisotropic gold nanoparticles showed promising potential in photothermal therapy (PTT) against cancer. The photothermal efficiency of anisotropic gold nanoparticles was determined in a study where hollow gold nanospheres (44 nm) exhibited an absorption peak at 808 nm, demonstrating their photothermal impact on mice at concentrations 100-fold lower than silica-coated iron oxide nanoparticles [93]. In addition to photothermal therapy, NIR has also been used for stimulus-dependent drug delivery at the target site. Jian You et al. (2010) demonstrated the dual role of hollow gold nanospheres (40 nm diameter) in enhancing photothermal implication and drug release under NIR irradiation [94]. The study also concluded that 63% more doxorubicin was loaded onto the polyethylene glycol (PEG)-coated hollow gold nanosphere. Besides the hollow nanosphere, nanoshells also exhibit properties favorable for theranostic application based on NIR absorption. The gold nanoshell consists of two components, one being an inner core and one an outer shell. Additionally, magnetic and high scattering properties were implemented on nanoshells by changing the core and replacing it with iron or silver [95,96]. The plasmonic properties of gold nanoshells towards the NIR region were tuned by varying thickness and diameter of the outer and inner layers, respectively [97,98]. In a typical study, Peng Huang et al. (2014) used liquid–liquid–gas, a three-phase approach, to synthesize multi-branched bellflower-shaped gold nanoparticles. Gold bellflower ( $\lambda_{\max}$  800 nm) showed high photothermal conversion efficiency (74%) with a powerful photoacoustic imaging effect under NIR laser irradiation [99]. In addition, the conjugation of gold nanorods enhanced the applicability of NIR light-responsive photothermal therapy by achieving target selectivity [100]. Table 2 [23–26,101–108] showed different anisotropic gold nanostructures used in cancer theranostics.

**Table 2.** Studies on using anisotropic gold nanoparticles in cancer nanotheranostics and their respective in vitro/in vivo safety assessment.

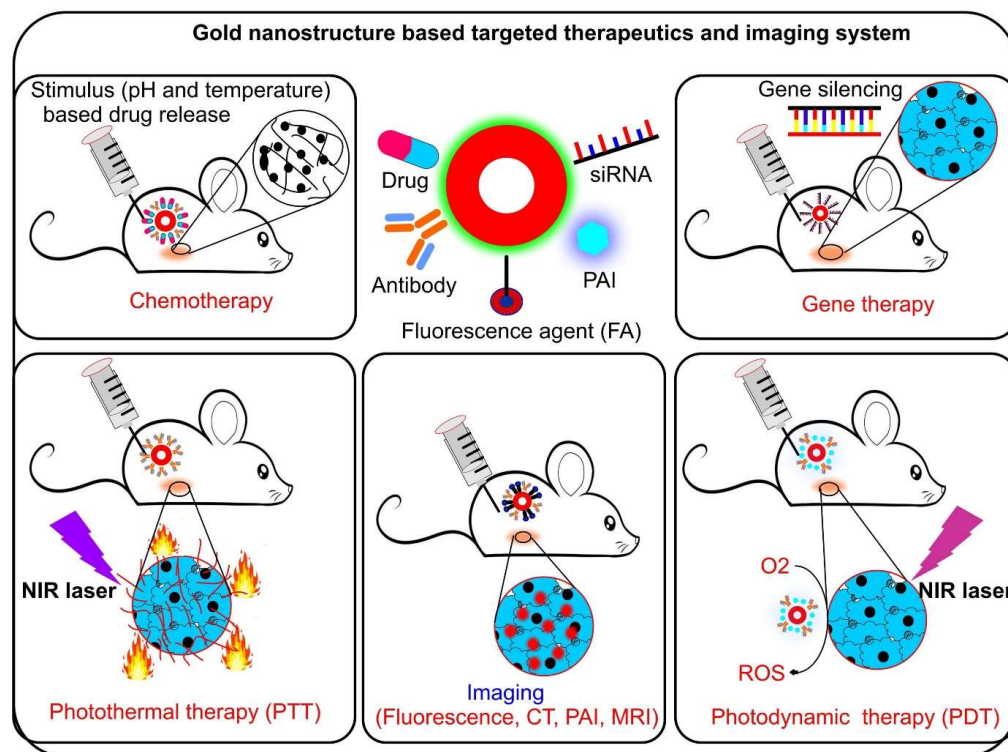
Gold Nanoparticles (Size/Shape)	Model System	Targeted Cancer	Therapy	Imaging/Modalities	Reference
Gold nanostars (25 nm)	MDA-MB-231, Bel-7402, MCF-7 cell lines and S180 tumor bearing mice	Cells over-expressed/under expressed integrins ( $\alpha_v\beta_3$ )	PTT	Fluorescence	[23]
PLGA-Gold nanoshell (115 nm)	HT-29 cells and HT-29 tumor-bearing mice	Colorectal cancer	PTT	MRI	[24]
Gold nanostars (70 nm)	Hela cells, MCF-7, breast tumor-bearing mice model	Breast cancer	PTT	Thermal sensing	[25]
Gold nanorods	SKOV3 and A549 cells, nude mice	Lung cancer	PTT	SPECT, CT	[26]
Gold Bellflowers (180 nm)	4T1, HeLa, SCC7 and CHO cells, nude mice	Breast cancer	PTT	Ultrasound, Photoacoustic	[99]
Liposome-Gold nanorods hybrid	4T1 and HT29	Breast cancer and colorectal cancer	Gene silencing	Multispectral optoacoustic tomography	[101]
Gold nanorods (10:40 nm)	MDA-MB-231 cell line	Breast cancer	NIR-PTT	Immunofluorescence	[102]
Gold-Silica Rattles (150 nm)	HeLa cells, CD1 mice	Human cervical cancer	PTT	Photoacoustic imaging, MRI, Fluorescence	[103]
Gold (20 nm) Gelatin shell (150 nm)	Glioma bearing mice	Glioma	Chemotherapy	Fluorescence	[104]

Table 2. Cont.

Gold Nanoparticles (Size/Shape)	Model System	Targeted Cancer	Therapy	Imaging/Modalities	Reference
Gold nanospheres (12 nm) and Gold nanostars (30 and 60 nm)	Mice with xenograft sarcomas	Sarcoma	PTT	SERS, CT and Two-Photon Luminescence	[105]
Gold nanorods (10:37 nm)	HeLa, mouse embryonic fibroblast cells (NIH-3T3), and tumor-bearing mice	Epithelial carcinoma	Photoacoustic	Photoacoustic Imaging	[106]
Gold nanorods (22:47 nm)	Panc-1 cells, Athymic nude mice (BALB/cASlac-nu)	Pancreatic carcinoma	PTT, chemotherapy, gene silencing	Fluorescence	[107]
PEI capped gold nanoparticles	PC-3	Prostate cancer	Gene silencing	Confocal	[108]

## 2.2. Surface Modification of Gold Nanostructures

The higher surface area to volume ratio rendered nanoparticles several advantageous surface functionalities. The higher drug loading and the assembly of multiple functional molecules are only possible using particles in the nano regime. In particular, gold nanoparticles have been engineered for theranostic purposes through surface modification such as capping or coating with drug/diagnostic molecules. Capping or coating also provide biocompatibility and stability to the nanoparticles in biological milieu. Surface modification is conducted by conjugating or labeling different functional moieties such as protein, antibody, amino acids, fluorescent dye, DNA, and siRNA onto nanoparticles for efficient therapy and detection [109–114]. The schematic representation of different functional moieties on an anisotropic gold nanoshell is shown in Figure 2. The various conjugated functional entities exhibit unique functionalities in cancer theranostics.



**Figure 2.** Diagram showing different functional entities; drug, antibody, siRNA and fluorescent agent capped around the gold nanostructure for cancer theranostic applications. The conjugation enhanced target selectivity and specificity for cancer therapies such as chemotherapy, gene therapy, photodynamic therapy, photothermal therapy, and imaging.



### 2.2.1. Enhanced Stability and Biocompatibility Using Cappings and Coatings

The pre-requisites for synthesizing gold nanoparticles include a precursor metal salt, a strong reductant, and a capping/stabilizing agent. The role of the capping agent is to provide colloidal stability to the nanoparticles. Gold nanoparticles of various shapes and sizes are synthesized using surfactants, polymers, polysaccharides, and biomolecules [55,115–118]. Among all, hexadecyltrimethyl ammonium bromide (CTAB) is the most frequently used surfactant, and is a well-established template imparting anisotropy in nanoparticles. The application of CTAB in synthesizing gold nanostructures of different shapes such as rods, triangles, star bipyramids etc., has been reported [119–122]. CTAB offers high stability to metallic nanoparticles under physiological conditions. The application of the surfactant based metal nanoparticles is limited to diagnostics/sensing/engineering. The inherent toxicity of the surfactant from the surface of metal nanoparticles hinders biological/clinical applications. In order to alleviate toxicity, the surfactant is coated/shielded by various biocompatible molecules on the metal gold surface. PEG is the most commonly used coating for biological use due to its non-toxic and biocompatible nature. For instance, thiolated PEG was used to coat CTAB-capped gold nanoparticles which resulted in the reduction in toxicity of the particles [123]. Other non-toxic or highly stable coatings, such as silica, have been used to coat gold nanorods with gold nanoclusters (AuNRs@SiO<sub>2</sub>@AuNCs) for their concurrent application in imaging, as well as photothermal treatment of cancer cells [124]. Similarly, a recent study reported the synthesis of hybrid plasmonic-luminescent nanomaterials, where silica encapsulated gold nanorods were functionalized with lipoic acid-capped silver nanocluster (Ag<sub>29</sub>(LA<sub>12</sub>)) and bovine serum albumin (BSA) capped gold nanocluster (Au<sub>30</sub> BSA), respectively [125]. Silica is known to increase the thermal efficiency of gold nanoparticles [126]. The coating of nanoparticles provides unique properties that augment their applicability in nanotheranostics. The selective binding of targeted functional moieties includes anticancer drugs, fluorescent tags, proteins, and antisense RNA for cancer treatment [108,109,111,127].

### 2.2.2. Functionalization and Conjugation for Target Specificity

The surface of gold nanoparticles has been modified using different coatings or cappings for their desired end-use. A diagnostic biosensor based on DNA (ERBB2c and CD24c) conjugated citrate-coated gold nanoparticles was developed for the early detection of breast cancer biomarkers [128]. The biosensor provided a brief indication of damage based on the increase and decrease in biomarker levels in biological fluid. However, to identify the exact target location of the lesion, various targeting moieties were conjugated to the gold nanoparticles for therapeutic and diagnostic purposes. The anticancer drug doxorubicin was loaded onto oligonucleotides conjugated to citrate-capped gold nanoparticles, and examined their therapeutic potential using a colon carcinoma cell line (SW480) [129]. Doxorubicin is a well-known broad-spectrum anticancer drug used to conjugate gold nanoparticles with different cappings showing multiple effects. Fucoïdan—a sulfated polysaccharide—was used as a reductant and a capping agent for synthesizing gold nanoparticles. These nanoparticles, after conjugation with doxorubicin, were used as nanocarriers for chemotherapy and photoacoustic imaging of breast cancer cells [130]. Multi-coated gold nanoparticles, such as citrate-capped gold nanoparticles coated with PEG 6000, followed by conjugation with the peptide-drug, efficiently increased antitumor activity and bioavailability, respectively [131]. The functionalization of these entities onto the nanoparticle surface was directly related to the nanoparticle size and shape. Similarly, 2-kDa-polyethyleneimine conjugated to gold nanoparticles was developed for efficient gene therapy in human corneal cells and the rabbit cornea. The conjugated gold nanostructures were selectively able to deliver genes in rabbits with minimum immune response. The study also showed a higher uptake of nanoparticles followed by their clearance [132]. A similar analysis of nanoconjugates showed that the peptide THRPPMWSPVWP was loaded onto the conjugated CLPFFD gold nanoparticle. The study concluded that gold nanoconjugates actively bound to the blood–brain barrier using translocating microvascular endothelial cells, and hence increased conjugate perme-

ability in the brain [133]. The study confirmed the efficient use of gold nanoconjugates in neurodegenerative therapeutic potential through in vivo and in vitro model systems.

### 3. Safety and Risk Assessment of Diverse Gold Nanostructures

The promising potential of various gold nanostructures for biological application (mainly theranostic-based) led towards deciphering and understanding their beneficial effects, along with their detrimental effects, on a biological system. The toxicological impact of gold nanostructures in a biological system is assessed using in vitro or in vivo model systems. The nanotheranostic applications involve safe and biocompatible nanomaterial for successful diagnosis and concurrent therapy with minimum side effects. The toxicity of gold nanostructures is determined primarily by their size, shape, surface chemistry, dose concentration, route of administration, and finally, their interaction with cellular components [134,135]. Nonetheless, the surface chemistry plays a critical role in determining the functionality of nanoparticles, and it also influences the toxicity outcome. As discussed earlier, the capping agent plays a major role in determining the surface chemistry of nanoparticles, rendering them with diverse functionalities. The widely used capping agent template for synthesizing anisotropic nanoparticles is hexadecyltrimethylammonium bromide (CTAB) [136]. The CTAB-assisted synthesis yielded gold nanoparticles of various shapes, such as spheres, rods, cubes, and prisms [137]. These various shaped CTAB stabilized gold nanoparticles showed shape-dependent toxicity in a prostate cancer cell line (PC3) (Figure 3). CTAB acts as an excellent structure-directing agent for synthesizing gold nanorods; however, they are highly toxic to in vitro and in vivo model systems [138]. Therefore, CTAB-capped nanoparticles were coated with PEG to achieve minimum toxicity, without affecting the physicochemical properties of the nanoparticles [139,140]. Additionally, PEG-coated gold nanoparticles offer strong biocompatibility of the nanoparticles due to their stealth nature when in the blood circulation [140]. It is also reported that bovine serum albumin (BSA), along with PEG effectively stabilizes gold nanoparticles in a size-controlled manner with increased biocompatibility [141]. However, from the reported studies, it is clear that nanoparticle toxicity is mainly dependent on various factors such as size, shape, and surface chemistry [142]. Surface chemistry of the nanoparticles plays a significant role in determining the nano–biointerface during their application. Therefore, in the case of gold nanoparticles that are inherently non-toxic, capping plays a major role in determining the safety of the nano-system. For example: CTAB-assisted nanoparticles are toxic, while PEG-capped nanoparticles are non-toxic in nature [138,143]. This is due to the change in surface chemistry. The toxicity assessments of different gold nanostructures using in vitro and in vivo model systems have been discussed elaborately in the following sections.

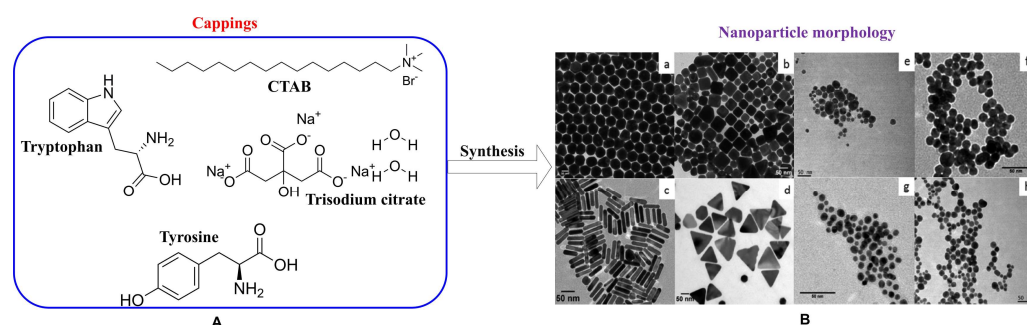
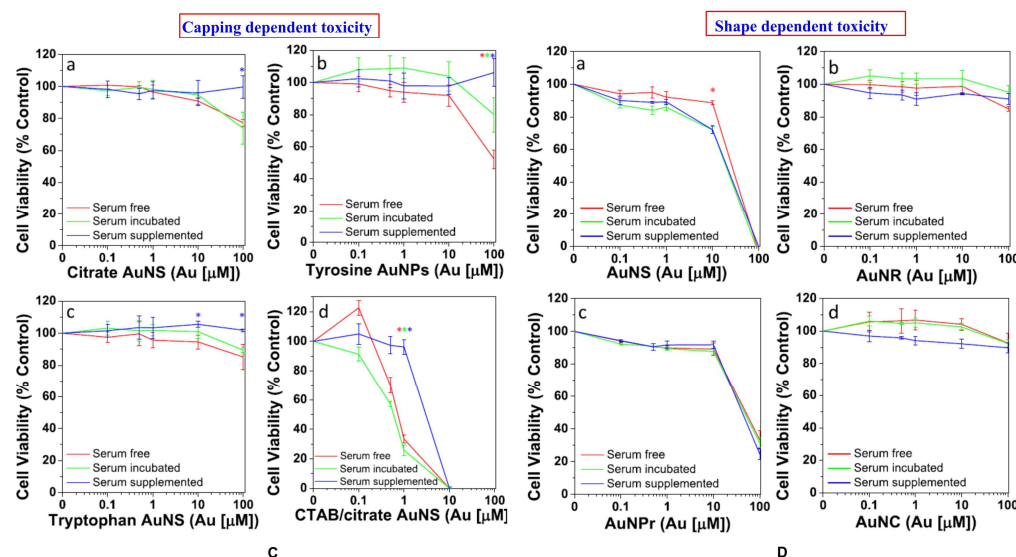


Figure 3. Cont.



**Figure 3.** (A) Representation of different cappings (CTAB, citrate, tryptophan, and tyrosine) used in synthesizing gold nanostructures of different shapes. (B) TEM images of (a) CTAB capped gold nanosphere, (b) CTAB capped gold nanocube, (c) CTAB capped gold nanorods, (d) CTAB capped gold nanoprism, (e) CTAB and citrate capped gold nanosphere, (f) citrate capped gold nanosphere, (g) tryptophan capped gold nanosphere, and (h) tyrosine capped gold nanosphere. (C) Cell viability was measured for gold nanosphere (AuNS) with various cappings: (a) citrate, (b) tyrosine, (c) tryptophan, and (d) CTAB and citrate in prostate cancer cells (PC3). (D) Cell viability was measured for different shapes of gold nanostructures capped via CTAB: (a) Gold nanosphere (AuNS), (b) gold nanorods (AuNR), (c) gold nanoprisms (AuNPr), and (d) gold nanocube (AuNC). Adapted from the ref. [137] with permission. Copyright@American Chemical Society. Asterisks indicate significant differences ( $p < 0.05$ ) between different conditions at the same dose point.

### 3.1. In Vitro Safety Assessment

The advent of gold nanostructures in cancer theranostics has been a boon towards rapid diagnosis, drug delivery, and effective therapeutic results. The property-based performance of the gold nanostructures is evaluated in vitro and in vivo prior to a clinical trial. The in vitro system is the preliminary test system to assess the toxicity of nanoparticles that are intended for biomedical applications. It is, however, too early to clearly define the absolute safety of nanoparticles, despite their use in NIR based theranostic applications [99,144]. The parameters such as particles' size, shape, surface chemistry, dosage concentration, and route of administration play critical roles in determining nanoparticle-mediated toxicity [145]. For example, gold nanospheres (45 nm) at a lower dose (10  $\mu\text{g/mL}$ ) showed higher toxicity compared to smaller particles (13 nm) at a higher dose (75  $\mu\text{g/mL}$ ) [146]. In addition, the use of anisotropic gold nanorods synthesized via a seedless method showed size-dependent toxicity in the HepG2 cell line [147]. Depending on the shape, sharp-edged nanoparticles such as nanoflowers and nanostars are more toxic when compared to spherical particles at the same lower concentrations [148,149]. It was also reported that sharp-edged nanoparticles tend to evade toxicity through endosome mediated delivery [150]. A study conducted by Diego Mateo et al. (2014) confirmed the cytotoxic nature of gold nanoparticles to the cell lines (HepG2 and HL-60) under certain conditions such as dose, exposure time, and size of the nanoparticles [151]. The study concluded that dose and time-dependent exposure to gold nanoparticles increased reactive oxygen species (ROS), decreased glutathione (GSH) and superoxide dismutase (SOD) activity in hepatocellular carcinoma (HepG2) and human leukemia (HL 60) cell lines, resulting in cytotoxicity and subsequent cell death. However, regardless of size, gold nanoparticles exhibited minimum or no toxic effects at an appropriate dose; for example, a dose that could be used for a therapeutic purpose. In addition to size, shape, and dose, surface chemistry also plays

an essential role in determining nanoparticle-mediated toxicity. The capping/stabilizing agent mainly governs the surface chemistry, which sometimes possesses both reducing and stabilizing properties. For example, in the case of glucose-capped gold nanospheres, glucose acts as both reducing and stabilizing agent. The glucose-capped gold nanoparticles showed non-toxic effects in HeLa cells, and were also used in cancer nanotheranostics [152]. These non-toxic cappings provide stability and biocompatibility of the nanoparticles that can be used for nano-based constructs in photothermal therapy and targeted drug delivery. The well-known trisodium citrate (TSC) capping is popular for its self-reducing, stabilizing properties, non-toxic behavior, size tunability, and ability to induce anisotropy in metal nanoparticles [153,154]. Additionally, a report contradicted the non-cytotoxicity nature of citrate-capped nanoparticles (15 nm) where these particles were found to cause cytotoxicity in HeLa and U937 cell lines, respectively [155]. A study confirmed that gold nanoparticles coated with citrate and polyamidoamine dendrimer (PAMAM) were genotoxic and cytotoxic when exposed to HepG2 and peripheral blood mononuclear cells (PBMC) at dose of 1  $\mu$ M and 50  $\mu$ M, respectively [156]. The nano-sized particles showed enhanced performance over micron-sized particles which can be attributed to an increased surface area to volume ratio [157]. Additionally, gold nanoparticles less than 2 nm are known for their inherent fluorescent property, which is used as a nanoprobe to diagnose disease states through real-time fluorescence-based imaging at the tumor site [158]. Despite the benefits of gold nanoclusters, toxicity has been a concern resulting in their limited application. For instance, a study reported cell death via necrosis or apoptosis upon exposure to particles of 1.4 nm or 1.2 nm, respectively [159]. To minimize the toxicity concern, a biocompatible coating such as GSH (tripeptide) was used to functionalize gold nanoclusters for real-time imaging in an in vitro system [160]. Similarly, cytotoxicity was controlled by coating the nanorods with mesoporous silica (mSiO<sub>2</sub>), poly(sodium 4-styrene sulfonate) (PSS), dense silica (dSiO<sub>2</sub>), PEG, and titanium dioxide (TiO<sub>2</sub>), and was validated through exposure to U-87 MG, MDA-MB-231, PC-3, HepG2, RAW 264.7, and HT-29 cells, respectively [161]. The study showed that mSiO<sub>2</sub> and PSS-coated gold nanorods showed significant toxicity, while PEG, dSiO<sub>2</sub>, and TiO<sub>2</sub> caused no cellular damage.

### 3.2. In Vivo Biodistribution and Toxicity Assessment

The complex structural assessment in an in vitro system is insufficient alone for the safety validation of nanoparticles intended for clinical application. In addition, in vitro toxicity assessment only shows the preliminary studies which are essential to correlate with an in vivo system that can guide the nanomaterials having theranostic potential towards clinical application. The in vivo model system is considered the next strata which is more close to humans' biological complexity or correlation, as compared to the in vitro system. The most commonly used in vivo model systems include zebrafish, *Caenorhabditis elegans*, *Drosophila melanogaster*, yeast, bacteria, rat, and mouse. These model systems enabled the study of the fate of nanoparticles from single-cell level to multicellular/tissue or organ system level [162,163]. The advantages of using these model systems are due to their complete genome sequencing, ease of maintenance, short lifespan, and functional homology to human genes [164]. The use of model organisms to assess the safety of nanomaterial (nanoparticles, nanoclusters) is currently a step towards using safer material for biomedical applications. Model organisms based on in vivo studies are also helpful in understanding the behavior and fate of gold nanoparticles in the living body. The gold nanoclusters accumulate primarily in the liver and spleen, resulting in further complexities leading to organ damage [165]. A study concluded that the administration of silver shelled gold nanorods to mice induced oxidative stress, and that the nanorods accumulated mainly in the target site and were later on found in other organs [166]. However, the fate of untargeted nanoparticles in the living body is destined to accumulate primarily in the liver and spleen [167]. The accumulation of nanoparticles in the liver is high due to the presence of Kupffer cells and macrophages that are responsible for the uptake of foreign materials, as gold nanoparticles are foreign to the cell, regardless of their size [168,169]. Therefore,



target specificity for theranostic-dependent therapy and diagnosis is a vital criterion for the treatment of any disease. According to a study by Lopez-Chaves et al. (2018), gold nanoparticles exhibited toxic effects upon exposure to three different sizes of nanoparticles (10 nm, 30 nm, and 60 nm) in Wistar rats. After sacrifice, traces of nanoparticles were found in the liver, intestines, urine, feces, kidneys, and spleen. The study revealed that smaller nanoparticles had a more deleterious effect on genetic material than cellular units, compared to larger nanoparticles [170]. A similar study by Schmid et al. (2017) confirmed that small gold nanoparticles showed higher circulation efficiency, wide biodistribution, and more toxic effects than larger nanoparticles [171]. In another study, the size-dependent distribution of gold nanoparticles was observed in which smaller particles selectively crossed the blood–brain barrier more efficiently [172]. The size of the particles in the nano regime enabled them to breach the blood–brain barrier, and provided a new avenue in diagnosis and targeted drug delivery. However, another comparative in vivo study regarding the fate of the nanoparticles of sizes 2 nm and 40 nm, respectively, was conducted. Interestingly, the nanoparticles were taken up, irrespective of size, by Kupffer cells in the liver and macrophages in other places. The smaller size (2 nm) was easily filtered through the kidneys and excreted through the urine after filtration [168]. In another study, *Drosophila* was used as an exposed model for gold nanoparticles at 12 ug/g; reduced fertility, life expectancy, DNA fragmentation, and upregulation of stress proteins were observed [173]. The previously mentioned studies in this section have elucidated the behavior of gold nanoparticles in various model organisms. Therefore, non-toxic gold nanostructures are considered as nanotheranostic tools in the treatment of multidimensional diseases such as cancer.

#### 4. Impact of Gold Nanostructures on Targeted Applications Related to Cancer Theranostics

##### 4.1. Diagnosis

Imaging technologies for diagnostic purposes have the advantage of allowing non-invasive collection of anatomical, functional, and molecular information. This information is used for targeted drug delivery, distribution, and mechanism of action [174]. Traditionally used imaging modalities are computed tomography (CT), magnetic resonance imaging (MRI), ultrasound (US), positron emission tomography (PET), photoacoustic tomography (PAT), single-photon emission computed tomography (SPECT), and fluorescence imaging [175]. Among the nanoparticles, gold nanoparticles are the first candidate used in the CT imaging of mouse organs and blood vessels [176]. Gold nanoparticles were used in conjugation with different functional entities for multi-model imaging. The selective and targeted specificity was achieved through surface functionalization with functional target molecules. Gold nanostructures are also used as a contrast agent in CT due to their X-ray attenuating properties and higher absorption capacity compared to conventional contrast agents [177]. On the other hand, gold nanoparticles have been modified with superparamagnetic iron oxide, gadolinium, and manganese to make them usable as contrast agents for MRI [178]. Imaging with fluorescent molecules is advantageous for rapid detection and for detailed information about the target site, and is low-cost and has multicolor imaging modalities (using different fluorophores). However, due to its low penetration ability, it is unsuitable for a diagnosis prescribed for clinical use. A multifunctional nanoconstruct (branched gold nanoshell) was developed by Antonio Topete et al. (2014) which has a central core of poly(lactic-co-glycolic acid (PLGA)-doxorubicin functionalized with human serum albumin (HSA), indocyanine green, and folic acid [179]. The study showed selective localization of the nanoconstruct in the tumor, and was retained for 48 h. The study also concluded that high fluorescence imaging was achieved due to NIR absorption of the nanoconstruct (particularly the gold nanoshell). A similar nanoconjugate based on nanostars was reported by Yang Liu et al. (2015), for nanotheranostics that were conjugated to different functional molecules for simultaneous use in CT, SERS, photothermal therapy, and imaging. The study concluded accumulation of nanoconjugates in the target tumor through imaging which showed a photothermal effect [105]. In addition, the study



also demonstrated continuous monitoring of controlled drug release at the specific site using the SERS mechanism in breast cancer cells (SK-BR-3). The drug release from the nanohybrid system and cancer cell viability were monitored by altering the SERS signal and cell viability assay, respectively [180]. The role of gold quantum dots in the theranostic approach was also realized and welcomed due to their smaller size as compared to nanoparticles. For example, gold quantum dots incorporated into mesoporous silica shells inhibited tumor growth significantly, as determined by NIR fluorescence, PAI, and MRI imaging methods [103]. Moreover, smaller particles are preferred for clinical use due to their higher clearance rate through the kidneys [181]. In a typical study, the magnetic property was harvested in gold nanoclusters, and was efficiently used in cancer diagnosis and treatment. Ultrasmall (1.4 nm) gold nanoclusters were synthesized using a virus as a template to target the T-cell receptor (TCR) in tumor cells. The study concluded excellent MRI and magnet-based hyperthermia for sub-cutaneous and deep-tissue tumors in live mice [182]. A comparative study between GSH-capped gold nanoclusters (2.5 nm) and a standard dye (IRDye 800CW) for fluorescence imaging confirmed superior fluorescence imaging performance in the nanocluster, with high accumulation and high clearance rate as compared to the standard [183] (Figure 4).

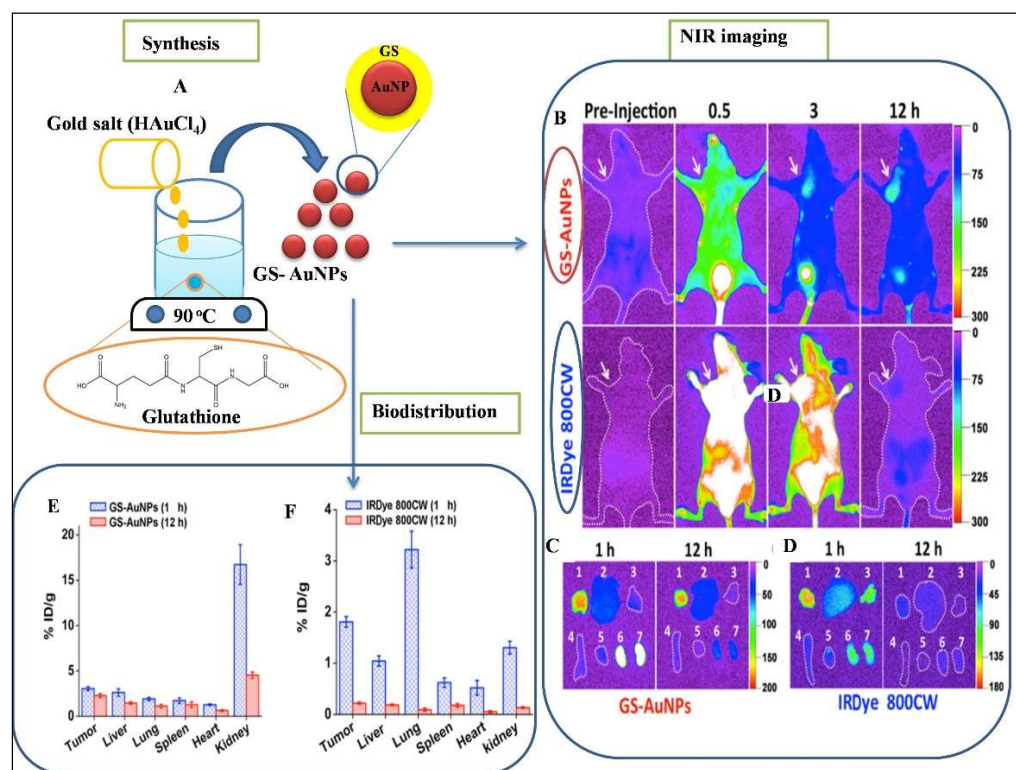


**Figure 4.** Gold nanocluster capped with glutathione (GS) (2.5 nm) for tumor imaging. (A) Gold nanocluster synthesis using GS as a capping agent. (B) NIR-dependent imaging in MCF tumor-bearing mice with glutathione capped gold nanocluster (GS-AuNCs) and standard dye (IRDye 800 CW) at the period of 0.5, 3, and 12 h. (C,D) showed ex vivo fluorescent images of organs and tumor removed at 1 and 12 h from the mice exposed to GS-AuNCs and IRDye 800CW, respectively. Labels: 1, tumor; 2, liver; 3, lungs; 4, spleen; 5, heart; 6, kidney (left); 7, kidney (right). (E,F) showed biodistribution of nanocluster and dye in different organs, respectively. Adapted from ref. [183] with permission. Copyright@American Chemical Society.

Ultra-small gold nanoparticles (5 nm) conjugated to dye showed strong NIR absorption and retained photoacoustic imaging capability similar to that of 40 nm particles [184]. In addition, these smaller nanoparticles showed a high clearance rate compared to larger ones in an in vivo model organism. The findings supported the use of small gold nanostructures

in photoacoustic imaging of cancer cells. Smaller gold nanoparticles also showed potential in PET technology by combining different functional entities such as GSH-stabilized gold nanoparticles (2.5 nm) conjugated to copper-64 ( $^{64}\text{Cu}$ ) for the assessment and diagnosis of renal function in mice [185]. In addition, small nanoparticles or nanoclusters have an advantage over large particles in terms of autofluorescence in the UV region [186]. The fluorescent emission property (from blue region to red region) of nanoclusters is tunable which is based on the number of binding atoms and emission of excitation light [186]. Autofluorescence of gold nanoclusters can be used for live-cell or tissue imaging. Arifin et al. (2011) reported that gadolinium-conjugated gold nanoparticles were used as a positive-contrast in ultrasound, CT, and MRI to visualize transplanted islet cells. The study concluded that gadolinium conjugated gold nanoparticles injected into mice resulted in normal blood glucose levels after seven days of injection [187].

#### 4.2. Targeted Therapeutics

The high surface area to volume ratio of gold nanostructures enabled a unique platform for labeling or coating multiple functional entities onto the nanoparticles' surface. These coatings or labels showed improved drug targeting, selectivity, biocompatibility, and the stability of nanoparticles. Various types of coating or capping have been used, including those with therapeutic value (DNA, peptides, proteins, siRNA), structure-directing agents (CTAB, citrate, anionic/non-ionic surfactants), targeting agents (antibodies), and polymers (PEG, PVP) [108,188–192]. Gold nanoparticles, due to their size, conveniently accumulate in cancer cells through leaky vasculature in the blood and lymphatic vessels. The EPR of the gold nanoparticles allows the conjugated drug to remain at the tumor site for a longer duration as compared to the drug when administered alone [193]. According to a few studies, nanoparticles of different sizes (<100 nm) passively accumulate in cancer tissue, providing higher drug loading at the target site. This results in less circulation of the drug in the blood leading to increased circulating half-life, thus preventing systemic toxicity [194,195]. However, the current strategy depends on the degree of vascularization and heterogeneous blood flow, limiting drug absorption and homogeneous distribution. The limitation is overcome by using vasoconstrictive drugs which narrow normal blood vessels and increase blood pressure. At the same time, cancer cells remain unaffected due to their abnormal vasculature, thereby improving the entry target of tumor cells [196]. In a study by Mykola Ya Spivak et al. (2013), gold nanoparticles (30 nm) were conjugated to levosimendan (SIMDAX)—a well-known cardioprotective drug—demonstrating its role in the treatment of heart failure in an in vivo model system [197]. Gold nanoparticles acted as nanocarriers to transport SIMDAX, and accumulated in infarcted arteries and capillaries of the endothelial layer. According to the finding, AuNP-SIMDAX and AuNP have significant cardioprotective effects in rats against doxorubicin-induced heart failure when compared to SIMDAX alone. The study also concluded that the intrapleural route of administration (local administration) showed the best effect compared to other assumed routes of administration, such as sonoporation and intravenous injection [197].

Gold nanoparticles conjugated with doxorubicin showed promising results in selective targeted therapy or diagnosis. The drug was released from gold nanoconjugates in a dose-dependent manner through specific stimulation of NIR laser irradiation. The design of nanoconjugates was also used for detection and treatment using a variety of functional molecules [198,199]. The doxorubicin being conjugated with different anisotropic nanoparticles, such as nanostars, nanoclusters, hollow nanospheres, and nanoshells has been reported [24,83,85,104]. These conjugated anisotropic nano-constructs showed the potency of doxorubicin in the NIR range with more minimal side effects than doxorubicin alone at the same dosage level [24,83,85,104]. Apart from doxorubicin, other antitumor drugs such as platinum-based drugs, camptothecin, irinotecan, and 5-fluorouracil were also conjugated to gold nanoparticles to achieve higher efficacy with minimum side effects upon exposure [75,82,200,201]. Camptothecin showed broad-spectrum anti-tumor activity by inhibiting topoisomerase 1, an enzyme responsible for unwinding DNA during replica-

tion [202]. However, camptothecin was highly toxic and less potent in showing anticancer activity compared to its natural derivative, 10-hydroxy camptothecin [203]. The anticancer potential of 10-hydroxy camptothecin was further enhanced through conjugation using gold nanoparticles [204].

The target selectivity of nanoparticles was found to be enhanced in the pathway of receptor–ligand mediated interactions, inducing intrinsic endocytosis and confirming the release of drug in cells [195]. Intrinsic endocytosis, also known as receptor-mediated endocytosis (RME), is responsible for the uptake of gold nanoparticles upon adsorption of surface proteins onto nanoparticles. RME involved clathrin-coated vesicles followed by the internalization of caveolae [205]. A study conducted by Nripen Chanda et al. (2010), as depicted in Figure 5, showed how peptide (bombesin) conjugated gold nanoparticles targeted the gastrin-releasing peptide (GRP) receptor. GRP is selective and only overexpressed in breast, prostate, and lung cancer cells [206]. Bombesins offered target specificity, while nanoparticles acted as nanocarriers for peptide delivery into the target cancer tissue.

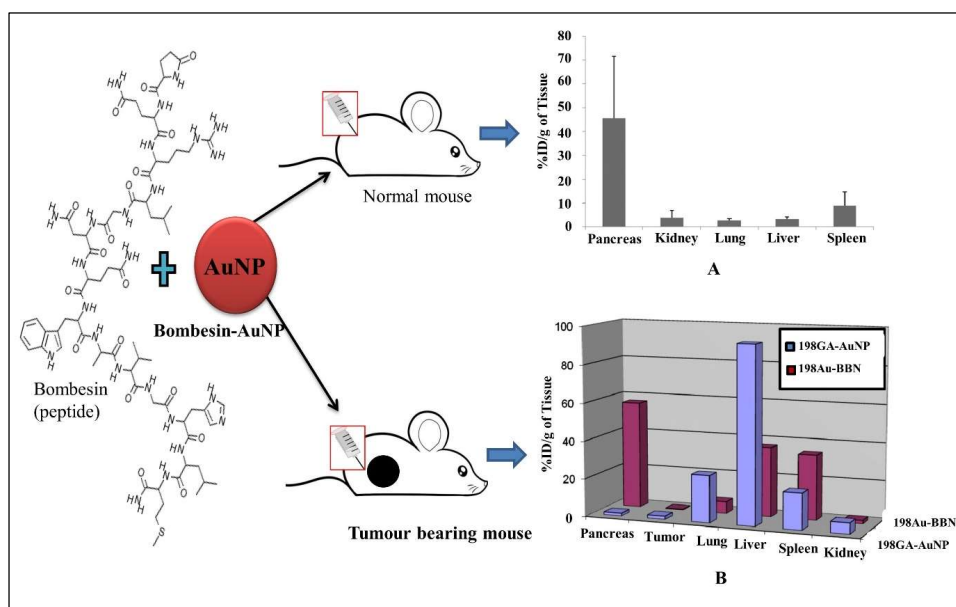


**Figure 5.** Bombesin-conjugated gold nanoparticles. (A) Concentration of conjugated nanoparticles in different organs after intraperitoneal administration in normal mice. (B) Comparison of bombesin (BBN) conjugated and gum arabic (GA) functionalized gold nanoparticle uptake after intraperitoneal administration in tumor-bearing mice. Selective uptake into the pancreas via the bombesin-specific receptor was observed. Adapted from ref. [206] with permission, PNAS.

Similarly, another peptide called arginylglycylaspartic acid (RGD) functionalized magnetoliposomes was used for its selective targeting of leaky vascular endothelial cells via the receptor  $\alpha v \beta 3$  integrin, an overexpressed receptor in cancer endothelial cells with significant accumulation at the tumor site [207]. A study reported that antibody-conjugated gold nanoparticles showed improved target specificity due to selective ligand–receptor interaction. Chung Hang J. Choi et al. (2010) reported conjugation of PEGylated gold nanoparticles with human transferrin antibodies to achieve selective targeting capability. The achieved selectivity also enhanced nanoparticle accumulation in targeted tumor cells [208]. The over-expressing protein, also known as a bio-marker, expressed on the cancer cell surface is used for targeting through conjugating antibodies to gold nanoparticles. Two of the most commonly used antibodies are against the epidermal growth factor receptor (EGFR) and the folate receptor: the most widely overexpressed proteins on cancer cell surfaces. These receptors are selectively targeted by designing specific antibody–nanoparticle conjugates against them [209,210]. In addition to the functional properties that result from conjugation and capping/coating, nanoparticles also ensure prolonged accumulation in cancer tissue

with a retention time of up to 72 h when administered intravenously [209]. The designed antibody–nanoparticle conjugates have been used in mice to assess therapeutic and diagnostic potential where nanoparticles have acted as carriers [80,210–212]. However, different targeting mechanisms are known, including passive (indirect) and active (direct) targeting. Passive targeting involves the use of nanoparticles coated/capped with therapeutic molecules which accumulate at the tumor site without any active transport. Furthermore, the lack of a normal lymphatic system in cancer tissue allows nanoparticles to remain for a longer duration. Passive targeting does not involve any specific targeting molecule. On the other hand, active targeting includes conjugating specific antibodies such as C225 to EGFR as cancer cell surface receptors [73,78,79]. In a study, the antibody (C225) conjugated nanoparticles showed higher uptake in EGFR-positive cells of mouse xenografts [79]. Overexpression of the receptor protein HER2 is prominent in breast and ovarian cancer cells against which branched gold nanoparticles were also antibody-conjugated [213]. Another commonly overexpressed receptor on the cancer cell surface is the folate receptor, which is necessary for the uptake of folic acid into the cell. Most ovarian carcinomas overexpress folic acid receptors, as shown in a previous study [214]. According to a previous report, folate-functionalized nanoparticles showed 4.7-fold higher accumulation in target tumors than their non-functionalized counterparts [82]. Therefore, the role of drug–folate conjugates can be exploited in preclinical studies for selective tumor targeting [215,216]. Table 3 described various targeting strategies of using gold nanoparticles in cancer theranostics, along with their advantages and disadvantages.

**Table 3.** Described various targeting moieties conjugated to gold nanoparticles for cancer therapy and diagnostics.

Targeting Strategies	Example	Advantages	Disadvantages	References
Cell-penetrating peptides (CPP)	Tat Peptide conjugated gold nanoparticles	<ul style="list-style-type: none"> <li>• CPP (mostly cationic) can penetrate the membrane and subsequently internalize into the cell</li> <li>• Low cytotoxicity due to their degradation into amino acids</li> </ul>	<ul style="list-style-type: none"> <li>• Low selectivity for first-generation CPP for cell, tissue, and organ</li> </ul>	[217–219]
Antibody targeted	C225 conjugated gold nanoparticles	<ul style="list-style-type: none"> <li>• Provide target specificity and selectivity</li> <li>• Higher uptake of nanoparticles due to EGFR receptor present in cancer cells</li> <li>• Can also load drugs over nanoparticles</li> </ul>	Lack of knowledge about the interaction between nanocarriers and biological systems, poor accumulation of nanoparticles at the tumor site, inadequate pharmacokinetics	[79,220]
Peptide-based	GRP-conjugated gold nanoparticles	<ul style="list-style-type: none"> <li>• Small size, low immunogenicity, lower manufacturing costs, increased efficiency for infiltrating tumor masses, high stability, and high tunability</li> </ul>	nonspecific uptake is still possible, especially if the target is expressed in healthy cells	[206,221]
Small molecules based	Folate-conjugated gold nanoparticles	<ul style="list-style-type: none"> <li>• Overexpression of folate receptor in cancer cells</li> <li>• Drug loading over nanoparticles for better efficiency</li> </ul>	<ul style="list-style-type: none"> <li>• Target-specific but widely distributed in different organs</li> </ul>	[222,223]



#### 4.3. Advanced Phototherapy

Photodynamic therapy (PDT) is a form of phototherapy that uses a light source and a photosensitizing chemical (agent) in conjugation with molecular oxygen to induce cell death through the generation of reactive oxygen species (ROS). Photosensitizers are exposed to the light of specific wavelengths leading to generation of nascent oxygen or free radicals. The wavelength depends on the selective absorption by the tumor tissue with enhanced selectivity through an increased ratio of targeted to non-targeted healthy tissue [224]. The anisotropic gold nanoparticles exhibit higher absorption properties at longer wavelengths. The improvement of the traditional PDT system in combination with gold nanoparticles reduced toxicity, increased efficiency, and improved cellular uptake by the cancerous cells [78,225]. Joseph D. Meyers et al. (2015) showed that gold nanoparticles selectively delivered labelled EGF and a photosensitizer PC-4 to the target tumor in vitro and in vivo, respectively. The in vitro study showed that epidermal growth factor peptide-targeted gold nanoparticles (EGF<sub>Prep</sub>-AuNPs)-PC4 selectively killed cancer cells two-fold more as compared to the PC-4 alone [78]. Interestingly, the in vivo study showed significant interruption in tumor development which was acquired through imaging. According to one of the studies, a nanoconstruct (Au@Polymer/MB-TF) was designed that consisted of gold nanoparticles, methylene blue (MB)—a photosensitizer, polystyrene-alt-maleic acid (PSMA)—a polymer for stabilization, and transferrin, for internalization using a light source (660 nm). The developed nanoconstruct showed minimum toxicity and induced apoptosis in cervical cancer cells [226]. Chen et al. (2018) conducted a study in which laser-assisted synthesized alkylthiolated gold nanoclusters were modified with human serum proteins (HSA) and catalase (CAT) demonstrating a multifunctional theranostic approach against cancer. The study concluded that gold nano-constructs selectively induced hypoxia and exhibited fluorescence with a high retention time in tumor tissues [227]. Gold nanodendrimer combined with zinc and phthalocyanine formed a Multiple Particle Delivery Complex (MPDC) which demonstrated efficient photodynamic therapy in a cancer cell line (MCF-7). Upon irradiation with the NIR laser (680 nm), an apoptosis-like feature with increased cytotoxicity, caspase activity, cell depolarization, and cytochrome C release was observed. In addition, BAX, BCL-2, CASP-2, and ULK-1 were also upregulated, leading toward programmed cell death [228].

Photothermal therapy is an enhanced treatment regime of photodynamic therapy in which cells are specifically sensitized and thermally damaged at a temperature of 45 °C using longer wavelengths of light. Anisotropic gold nanoparticles such as nanorods, nanoshells, and nanocages have been used in photothermal therapy owing to their longer wavelength (NIR-IR) plasmonic absorption which converts light energy into thermal energy [229,230]. Yang-Liu et al. (2015) synthesized gold nanorods using a seed-mediated approach, followed by coating with mesoporous silica, and combining PEG, tLYP-1 peptide, and indocyanine green (ICG). In addition, the synthesized nanorods were stable in aqueous media due to silica coating, thereby facilitating endocytosis of tLYP-1 and ICG. Fluorescence imaging and phototherapy in breast cancer cell lines were achieved through NIR irradiation [230]. Similarly, a study reported the functionalization of gold nanorods using poly-L-glutamic acid (PGA), cisplatin, and folic acid for the therapeutic purpose [231]. PGA provided biocompatibility; cisplatin as a chemotherapeutic agent and folic acid for targeted release of cisplatin were conjugated to nanorods (Figure 6). A synthesized nanoconjugate (FA-GNR@Pt) was administered systemically and combined with localized NIR laser irradiation, which resulted in significant tumor growth inhibition in triple-negative breast cancer [231]. Weijun Xu et al. (2019) showed a gold nanorod synthesized from functional hyaluronic acid, conjugated with anti-HER2 antibodies, 5-aminolevulinic acid (ALA), and Cy7.5 for active targeting, photodynamic therapy, and fluorescence imaging, respectively. The study confirmed the dual-targeting mechanism of selective uptake by HER2 and CD44. The combined effect of PDT/PTT upon NIR laser irradiation was able to destroy breast cancer cells (MCF-7) significantly, as compared to PDT or PTT alone [232]. In another study, gold nanorods were reactivated with pegylated mesoporous silica (SiO<sub>2</sub>), a photosensitizer



(Ce6), and cell-penetrating D-type peptide (D-CPP). The combined nanoconstruct (Ce6-D-CPP) induced cytotoxicity and apoptosis in cancer cells (MCF-7), and MCF-7 xenograft in nude mice [233]. Similarly, mesoporous silica-coated gold nanorods (AuNR@MSN) have been developed for photodynamic and photothermal therapy. Indocyanine green (ICG), cyclodextrin (CD-CD), and peptide RLA ([RLARLAR]<sub>2</sub>) were conjugated to AuNR@MSN. The conjugated peptide conferred membrane permeability and selectively targeted cancerous tissue. The synthesized nano constructs showed hyperthermia in in vivo and in vitro model systems where ROS generation was observed [234]. Ling-Yu Bai et al. (2015) developed a nanocomposite composed of hollow gold nanospheres and superparamagnetic iron oxide nanoparticles. The NIR absorption property of hollow gold nanospheres combined with iron oxide's magnetic properties provided a platform for theranostic cancer application through simultaneous imaging and photothermal therapy [235].

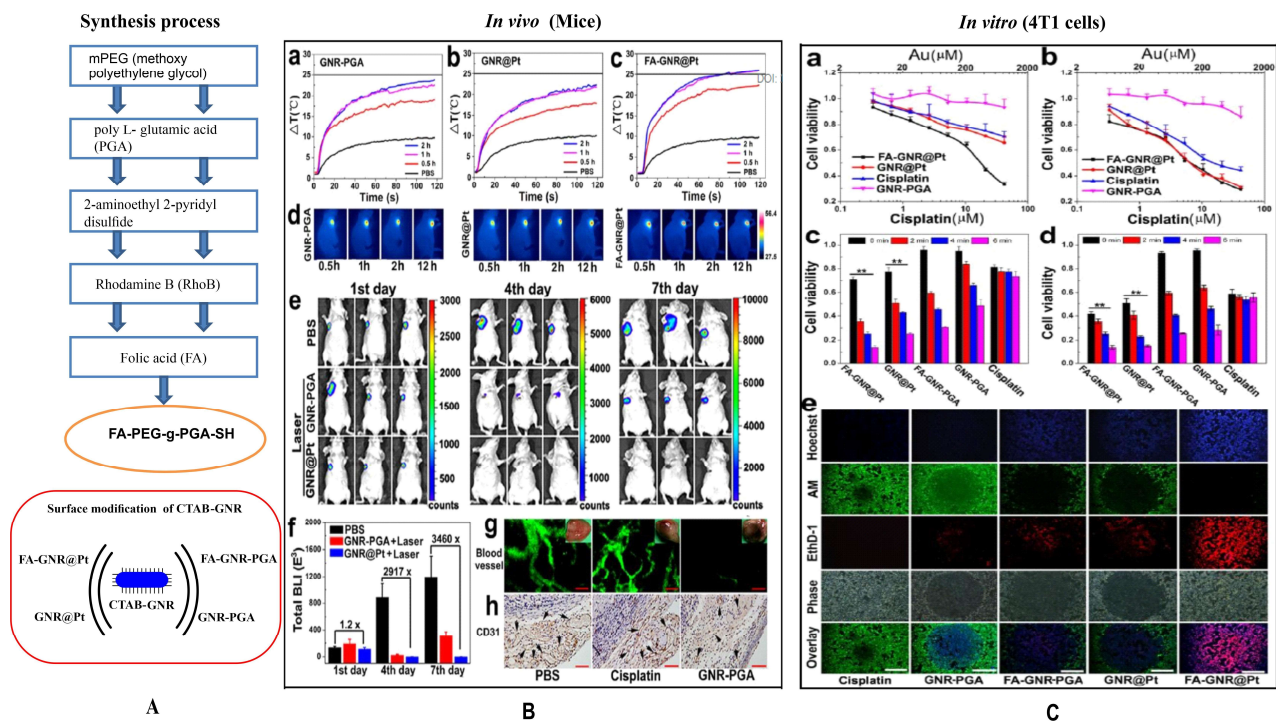


**Figure 6.** Gold nanorods coupled with various functional moieties for in vivo and in vitro photothermal treatment. **(A)** Surface modification of CTAB-GNR with folic acid (FA), cisplatin (Pt), and poly-L-glutamic acid (PGA) to synthesize thiolated poly (ethylene glycol)-graft-poly (L-glutamic acid) copolymers with FA modification (FA-PEG-g-PGA-SH). **(B)** In vivo hyperthermia impact and photothermal ablation of tumor blood vessels (**a–d**). (**a–c**) heat liberation capacity of GNR-PGA, GNR@Pt, and FA-GNR@Pt, respectively; (**d**) representative images of NIR laser-irradiated mice at various time intervals post-injection; (**e**) laser irradiated images of whole-body mice treated with GNR@Pt, GNR-PGA, and PBS on day 1, 4, and 7, respectively; (**f**) graphical representation of bioluminescence imaging (BLI) intensity after laser irradiation; (**g**) image showing tumor blood vessels perfusion. PBS, cisplatin and GNR-PGA nanoparticles; (**h**) micro vessel density estimation (MVD) of blood vessels stained with CD-31 antibody on the 7th day after laser irradiation. **(C)** Cytotoxicity assessment of GNR@Pt on 4T1 cells. (**a,b**) showed cytotoxicity of FA-GNR@Pt, GNR@Pt, cisplatin, or PGA-GNR on 4T1 cells post 4 h and 24 h incubation, respectively; (**c,d**) cell viability assessment of 4T1 cells after 4 h and 24 h, respectively, upon exposure to FA-GNR@Pt, GNR@Pt, cisplatin, or PGA-GNR; (**e**) 4T1 cells were treated with GNR@Pt and laser irradiation to perform a live-apoptosis-dead staining experiment. Adapted from ref. [231] with permission.

#### 4.4. Gene Therapy

The discovery of drug molecules and their preclinical studies focuses on future issues which affect the drug's efficacy, biocompatibility, limited solubility, dose concentration, non-specificity of the target, bioavailability, and short half-life in circulation [236]. The translational potential of nanoparticles increases the potency of drugs and biomolecules that are functionalized to them. The designed nanoparticle's potential enabled the development of disease-specific theranostic systems that can reduce healthcare costs and time with simultaneous diagnosis and treatment. These therapeutic and diagnostic tools are simply a unit of gold nanoparticles and small drug molecules—a peptide, protein, or antibodies, a ribozyme, and antisense nucleotides (siRNA, miRNA, snRNA) [237]. Modern therapies include gene therapy or gene silencing therapy, which promise a potent solution to fight against cancer. Gene therapy works on down-regulating the signaling pathways involved in the overexpression of genes that are responsible for altering the cellular protein levels leading to cancer. For example, in gene therapy, it has been found that siRNA (small interfering RNA) downregulates the expression of a particular gene in cancer cells [238]. Despite this, siRNA mediated gene therapy is not popular due to its short half-life. This is because RNAase activity in the cell system affects its stability and is very reactive; thereby it is considered as an obstacle to theranostic applications. This shortcoming is overcome by introducing nanoparticles in the domain of gene therapy. For example: AuNPs are used as nanocarriers in gene silencing strategies for overexpressed cancer genes, evading siRNA-mediated gene delivery [239–241]. Several studies on using AuNPs of different shapes and sizes for targeted gene silencing in cancer cells have also been reported [242,243]. In a typical study, Wei Lu et al. (2010) used hollow gold nanospheres for selective siRNA delivery to the tumor site. The synthesized siRNA can selectively bind nuclear factor kappa B (NF- $\kappa$ B) and decrease its expression through folate receptor-mediated endocytosis. The NF- $\kappa$ B protein complex regulates DNA transcription, cytokine secretion, and cell viability [82]. The study confirmed siRNA's selective, specific delivery and safe release from conjugated hollow gold nanospheres after NIR irradiation at the tumor site. It was also found that the combined therapy of photothermal transfection of nano-constructs induced apoptosis and delayed tumor development. Concomitantly, it was observed that the liver, spleen, kidneys, and lungs were unaffected, despite the accumulation of nanoparticles in these organs. Gold nanoparticles exhibiting NIR absorption (nanorods and nanoshells) showed high efficiency in photothermal transfection, imaging, hyperthermia, and targeted drug delivery [101,107,243,244]. Gold nanoparticles, particularly gold nanorods, have been used to simultaneously deliver two molecules: doxorubicin and the siRNA of Kirsten rat sarcoma virus (KRAS) gene. The concomitant release of both molecules provided a synergistic effect and subsequently reduced tumor growth in an in vivo model system [107].

Similarly, spherical gold nanoparticles have also been used for effective siRNA targeting and delivery in other model systems such as cell lines, hydra, and mice. The study reported 65% of c-MYC gene silencing [245,246]. Furthermore, it was observed that covalently bound siRNA was more effective than ionized siRNA adsorbed on the surface of nanoparticles. Similarly, besides siRNA, other molecular components have also been used to inhibit specific gene expression. For example, single-stranded DNA (ssDNA) is selectively delivered to the target site using AuNPs as nanocarriers to silence various RNA-mediated processes in the cell [242,247,248]. The emergence of new technologies, such as the gold nanoparticle-based molecular beacon system, have been developed for determining miRNA expression responsible for over-expression of the undesired proteins. The beacon system uses a fluorescent-based detection method. Nevertheless, the toxicity of the fluorescence-based system was characterized in vitro and in vivo prior to therapeutic application [247–249]. The nano beacon system has also been used to overcome multiple drug resistance: a serious concern associated with cancer treatment while using drugs only.

## 5. Improved Clinical Outcomes in the Field of Nanotheranostics

The first clinical study with AuNPs was performed on solid tumors with effective targeting through conjugation of TNF to nanoparticles. Gold nanoparticles (27 nm) were coated with PEG; conjugated to the target molecule rhTNF; and administered to 30 patients at fixed doses, which showed high efficacy without compromising safety [250]. A pilot study on treating head and neck and lung cancer using gold nanoshells (also called Au-roshells) via phototherapy was conducted which showed promising results [251,252]. The Au-roshells were systemically infused, passively deposited in target lesions, and irradiated with a laser. Another study reported the treatment of gliosarcoma using gold nanoparticles functionalized with small nucleic acids (SNA) and a drug NU-0129. The study concluded that AuNP-SNA-NU-0129 selectively crossed the blood–brain barrier and reached the target site Bcl2L12—the gene responsible for the development of tumor growth by preventing apoptosis. The study reported complete tumor resection within 8–48 h after intravenous administration [253]. Haitham Amal et al. (2016) conducted a study with 484 participants using gold nanoparticles to detect gastric cancer. The exhaled alveolar air samples were collected from subjects via endoscopy using Tedlar bags (Keika Ventures, LLC). The collected samples were analyzed using gold nanoparticles and compared with the samples run on a standard technique: gas chromatography coupled mass spectrometry (GC-MS) [254]. In a recent study, Ardeshir R. Rastinehad et al. (2019) conducted a pilot clinical trial in prostate tumor-bearing patients using NIR induced phototherapy with silica coated gold nanoshells for the treatment [255].

## 6. Opportunities and Challenges in Cancer Nanotheranostics

The use of various nanomaterials with desirable properties and recent advances in theranostic approaches have revealed inevitable hiccups in cancer therapy and care. The development of effective anticancer nanotherapeutics remains a significant challenge, as only a few nanoformulations have entered clinical trials. The physicochemical properties of nanoparticles play an essential role in their use for cancer theranostics, such as their biocompatibility and stability [256]. Furthermore, the nanoparticles administered can interact with biomolecules or ions in the biological milieu to form aggregates affecting the efficiency of the nanoformulation, making them ineffective in tumor destruction [257]. In regard to biological application, the storage and stability of nanoparticles also affect their pharmacological performance [258,259]. Nanocarriers in cancer theranostics can also have unintended consequences due to unpredictable complex interactions with biological entities [260]. Apart from metal gold nanostructures, there are also reports on toxicity from other nanomaterials due to their high aspect ratios [261,262]. Although, it has been reported that gold nanoparticles are inherently non-toxic, their functionality for the intended application is determined by the capping molecules. Therefore, it is important to discern the toxicity of the nanoparticles capped with different ligands or capping agents. For example, cationic molecules such as CTAB cause toxicity compared to their anionic counterpart in vitro [263]. This is because the cell membrane is negatively charged, due to the presence of phospholipids, which shows electrostatic interaction with the opposite charge resulting in membrane disruption. Another equally important aspect is considering how the conjugated ligands change the pharmacokinetics, biodistribution, and eventual side effects upon exposure to the cells. However, a conclusive mechanism of interaction between the capped molecule and the biological system is yet to be established. Additionally, clinical translation is confronted with a significant barrier in the commercialization of nanomedicine, alongside the issues with large-scale synthesis and cost-effectiveness. In general, chemoresistance and the heterogeneity among cancer cells hinder certain therapeutics, which is why they are not successful in the majority of patients [264]. In this case, a strategy to overcome tumor heterogeneity is to target stromal cells. Stromal cells are the supportive tissue that provides support and nutrients to the lymphatic system. By tagging nanoparticles with stromal antagonists, it is possible to greatly increase the effectiveness of anti-cancer therapeutics. Further investigation is warranted to reveal novel molecular

targets that are only expressed in the tumor microenvironment, which aids targeting efficiency of the nanoparticle-based therapy. Cancer stem cells (CSC) or cancer initiating cells (CICs) are also important candidates for drug targeting by eradicating CSCs/CICs chemoresistance, and possibly eliminating tumor reoccurrence. However, characterization of the systemic performance of gold nanoparticles in vivo is essential for advancing the future of nanomedicine [264]. Each multifaceted nanoparticle system is unique and must be evaluated independently. Systematic studies on toxicity, pharmacokinetics, and efficacy need to be carried out under precise conditions before developing nanomedicine. Figure 7 depicted the various challenges associated with the use of gold nanostructures in cancer theranostics.

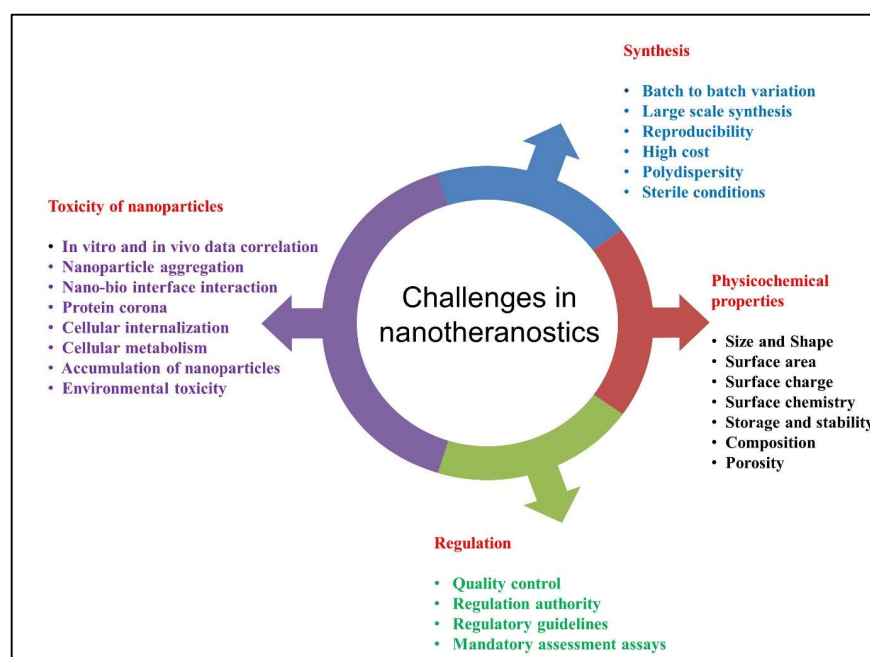


**Figure 7.** Challenges associated with nanotheranostics for reaching from lab to clinic; the spectra of challenges include synthesis, controlled physico-chemical properties, safety, and regulations.

## 7. Conclusions and Future Outlook

The need of the hour is to improve the life of cancer patients by providing early medical interventions through modern treatment facilities. One of the emerging areas is theranostics, which plays a crucial role in providing novel strategies and capabilities for the early-stage detection and treatment of cancer. Theranostics coupled with smart multifunctional nanomaterials, especially gold nanostructures, has paved the way towards developing a robust platform for clinical applications. This was due to the superior optical properties tuning from the visible to the NIR/IR wavelengths. The excellent optical features, along with isotropic and anisotropic behavior of gold nanoparticles, enabled the destruction of cancer cells via PTT/PDT. In this review, the authors mainly focus on the advancements in nanotheranostics in the past decade, and its role in cancer therapeutics using gold nanostructures. The potential of gold nanoparticles in various cancer therapeutics and diagnoses depends on the size, shape, surface complexity, conjugated functional entities, dose concentration, and route of administration. The target selectivity and specificity of gold nanostructures to the tumor site were achieved through binding molecules based on the target of interest. Tailored shapes of gold nanostructures (nanorods, nanoshells, nanocages, hollow nanospheres, and nanostars) exhibit absorbance in the NIR region, which is considered to be the optical therapeutic window. These tunable plasmonic properties of gold nanoparticles showed improved therapeutic potential in killing tumor cells via photothermal and photodynamic therapy, allowing the generation of heat and reactive



oxygen species (ROS), respectively. When considering the smaller atomic sizes, gold nanoclusters possess an intrinsic fluorescent property which does not quench compared to traditionally used fluorescent nanoparticles or dyes. The capability of various sizes of gold nanostructures has gained tremendous attention in nano-optic-based therapeutics, along with nanophotonics and theranostics applications involving laser-guided approaches.

This review elaborated on the gold nanostructure's potential for providing non-invasive and minimally invasive imaging modalities with precise targeting capability. However, the use of theranostics for clinical applications has several challenges in terms of repeatability, owing to the discrepancies in the *in vitro* and *in vivo* animal studies, and further human clinical trials. However, there are very few clinical trials on the progress of nanotechnology based cancer treatment. The transformation of the lab to bench technologies will lead to new frontiers in developing nanotheranostic strategies and approaches for identifying pathological conditions triggering various disease conditions. The compilation of studies in this review will aid the understanding of the complexities of nanotheranostics, and put forward a road map in bringing it from lab to clinic. Furthermore, the challenges of manufacturing nanoparticles with less toxicity, and providing stable nanoparticles with detailed characterization, will help to determine their efficient use in theranostics.

To date, there are no commercialized or FDA-approved theranostic nano-based therapeutic agents due to the nanoparticle's complex surface chemistry, and several other associated challenges. These include synthetic routes, multifunctional capping agents, conjugation (electrostatic/covalent), and strategies of drug payload to deliver at the target site with precision. *In vivo*/*In vitro* studies are challenging tasks for data correlation and require consensus for reproducible results to correlate the efficiency of different nanoparticles.

This review aims to disseminate the efforts made in the area of nanotheranostics and cancer in the past decade. However, realizing their impacts on treating and detecting cancer requires a collective effort from multidisciplinary researchers, involving chemists, physicists, biologists, engineers, policy decision-makers, and regulatory agencies to bring the lab scale developments to the commercial scale for the welfare of human health.

**Author Contributions:** Conceptualization provided by A.K., and R.G.R., A.K., N.D. and R.G.R. contributed towards the writing of the review content and structuring of the manuscript. All authors have read and agreed to the content of the manuscript.

**Funding:** This research received no external funding.

**Acknowledgments:** The authors acknowledge the Council for Scientific and Industrial Research (CSIR), New Delhi, India, for providing fellowship, and CSIR-IITR for providing the facilities and infrastructure. The manuscript was approved by the CSIR-IITR Institutional Publication Committee and granted the communication number- IITR/SEC/MS/2022/52.

**Conflicts of Interest:** The authors declare no conflict of interest.

## References

1. Sung, H.; Ferlay, J.; Siegel, R.L.; Laversanne, M.; Soerjomataram, I.; Jemal, A.; Bray, F. Global cancer statistics 2020: GLOBOCAN estimates of incidence and mortality worldwide for 36 cancers in 185 countries. *CA Cancer J. Clin.* **2021**, *71*, 209–249. [[CrossRef](#)] [[PubMed](#)]
2. Abbas, Z.; Rehman, S. An overview of cancer treatment modalities. In *An Overview of Cancer Treatment Modalities*; Shahzad, H.N., Ed.; IntechOpen: London, UK, 2018; Volume 1.
3. Holmberg, C.J.; Katsarelias, D.; Jespersen, H.; Carneiro, A.; Elander, N.O.; Helgadottir, H.; Isaksson, K.; Jansson, M.; Wirén, S.; Ullenhag, G.J. Surgery of metastatic melanoma after systemic therapy—The SUMMIST trial: Study protocol for a randomized controlled trial. *Acta Oncol.* **2021**, *60*, 52–55. [[CrossRef](#)] [[PubMed](#)]
4. Lammers, T.; Kiessling, F.; Hennink, W.E.; Storm, G. Drug targeting to tumors: Principles, pitfalls and (pre-) clinical progress. *J. Control. Release* **2012**, *161*, 175–187. [[CrossRef](#)] [[PubMed](#)]
5. Jagtap, P.; Sritharan, V.; Gupta, S. Nanotheranostic approaches for management of bloodstream bacterial infections. *Nanomedicine* **2017**, *13*, 329–341. [[CrossRef](#)]
6. Chen, Q.; Du, Y.; Zhang, K.; Liang, Z.; Li, J.; Yu, H.; Ren, R.; Feng, J.; Jin, Z.; Li, F. Tau-targeted multifunctional nanocomposite for combinational therapy of Alzheimer's disease. *ACS Nano* **2018**, *12*, 1321–1338. [[CrossRef](#)]



7. Kim, H.J.; Lee, S.M.; Park, K.H.; Mun, C.H.; Park, Y.B.; Yoo, K.H. Drug-loaded gold/iron/gold plasmonic nanoparticles for magnetic targeted chemo-photothermal treatment of rheumatoid arthritis. *Biomaterials* **2015**, *61*, 95–102. [\[CrossRef\]](#)
8. Zhou, M.; Hou, J.; Zhong, Z.; Hao, N.; Lin, Y.; Li, C. Targeted delivery of hyaluronic acid-coated solid lipid nanoparticles for rheumatoid arthritis therapy. *Drug Deliv.* **2018**, *25*, 716–722. [\[CrossRef\]](#)
9. Jung, E.; Kang, C.; Lee, J.; Yoo, D.; Hwang, D.W.; Kim, D.; Park, S.-C.; Lim, S.K.; Song, C.; Lee, D. Molecularly engineered theranostic nanoparticles for thrombosed vessels: H<sub>2</sub>O<sub>2</sub>-activatable contrast-enhanced photoacoustic imaging and antithrombotic therapy. *ACS Nano* **2018**, *12*, 392–401. [\[CrossRef\]](#)
10. Kim, T.; Zhang, Q.; Li, J.; Zhang, L.; Jokerst, J.V. A gold/silver hybrid nanoparticle for treatment and photoacoustic imaging of bacterial infection. *ACS Nano* **2018**, *12*, 5615–5625. [\[CrossRef\]](#)
11. Tian, Q.; Price, N.D.; Hood, L. Systems cancer medicine: Towards realization of predictive, preventive, personalized and participatory (P4) medicine. *J. Intern. Med.* **2012**, *271*, 111–121. [\[CrossRef\]](#)
12. Park, S.; Jung, U.; Lee, S.; Lee, D.; Kim, C. Contrast-enhanced dual mode imaging: Photoacoustic imaging plus more. *Biomed. Eng. Lett.* **2017**, *7*, 121–133. [\[CrossRef\]](#) [\[PubMed\]](#)
13. Chen, X.; Wong, S.T. Cancer theranostics: An introduction. In *Cancer Theranostics*; Elsevier: Amsterdam, The Netherlands, 2014; pp. 3–8.
14. Fricker, S.P. Medical uses of gold compounds: Past, present and future. *Gold Bull.* **1996**, *29*, 53–60. [\[CrossRef\]](#)
15. Vlamidis, Y.; Voliani, V. Bringing again noble metal nanoparticles to the forefront of cancer therapy. *Front. Bioeng. Biotechnol.* **2018**, *6*, 143. [\[CrossRef\]](#)
16. Hu, X.; Zhang, Y.; Ding, T.; Liu, J.; Zhao, H. Multifunctional gold nanoparticles: A novel nanomaterial for various medical applications and biological activities. *Front. Bioeng. Biotechnol.* **2020**, *8*, 990. [\[CrossRef\]](#) [\[PubMed\]](#)
17. Hammami, I.; Alabdallah, N.M. Gold nanoparticles: Synthesis properties and applications. *J. King Saud Univ. -Sci.* **2021**, *33*, 101560. [\[CrossRef\]](#)
18. Vechia, I.C.D.; Steiner, B.T.; Freitas, M.L.; dos Santos Pedroso Fidelis, G.; Galvani, N.C.; Ronchi, J.M.; Possato, J.C.; Fagundes, M.Í.; Rigo, F.K.; Feuser, P.E. Comparative cytotoxic effect of citrate-capped gold nanoparticles with different sizes on noncancerous and cancerous cell lines. *J. Nanopart. Res.* **2020**, *22*, 1–11. [\[CrossRef\]](#)
19. Sau, T.K.; Pal, A.; Jana, N.; Wang, Z.; Pal, T. Size controlled synthesis of gold nanoparticles using photochemically prepared seed particles. *J. Nanopart. Res.* **2001**, *3*, 257–261. [\[CrossRef\]](#)
20. Niu, J.; Zhu, T.; Liu, Z. One-step seed-mediated growth of 30–150 nm quasispherical gold nanoparticles with 2-mercaptosuccinic acid as a new reducing agent. *Nanotechnology* **2007**, *18*, 325607. [\[CrossRef\]](#)
21. Perrault, S.D.; Chan, W.C. Synthesis and surface modification of highly monodispersed, spherical gold nanoparticles of 50–200 nm. *J. Am. Chem. Soc.* **2009**, *131*, 17042–17043. [\[CrossRef\]](#)
22. Liu, X.; Xu, H.; Xia, H.; Wang, D. Rapid seeded growth of monodisperse, quasi-spherical, citrate-stabilized gold nanoparticles via H<sub>2</sub>O<sub>2</sub> reduction. *Langmuir* **2012**, *28*, 13720–13726. [\[CrossRef\]](#)
23. Chen, H.; Zhang, X.; Dai, S.; Ma, Y.; Cui, S.; Achilefu, S.; Gu, Y. Multifunctional gold nanostar conjugates for tumor imaging and combined photothermal and chemo-therapy. *Theranostics* **2013**, *3*, 633. [\[CrossRef\]](#) [\[PubMed\]](#)
24. Jing, L.; Liang, X.; Li, X.; Lin, L.; Yang, Y.; Yue, X.; Dai, Z. Mn-porphyrin conjugated Au nanoshells encapsulating doxorubicin for potential magnetic resonance imaging and light triggered synergistic therapy of cancer. *Theranostics* **2014**, *4*, 858. [\[CrossRef\]](#) [\[PubMed\]](#)
25. Wang, S.; Teng, Z.; Huang, P.; Liu, D.; Liu, Y.; Tian, Y.; Sun, J.; Li, Y.; Ju, H.; Chen, X. Reversibly extracellular pH controlled cellular uptake and photothermal therapy by PEGylated mixed-charge gold nanostars. *Small* **2015**, *11*, 1801–1810. [\[CrossRef\]](#)
26. Jang, B.; Park, S.; Kang, S.H.; Kim, J.K.; Kim, S.-K.; Kim, I.-H.; Choi, Y. Gold nanorods for target selective SPECT/CT imaging and photothermal therapy in vivo. *Quant. Imaging Med. Surg.* **2012**, *2*, 1. [\[PubMed\]](#)
27. Pérez-Juste, J.; Pastoriza-Santos, I.; Liz-Marzán, L.M.; Mulvaney, P. Gold nanorods: Synthesis, characterization and applications. *Coord. Chem. Rev.* **2005**, *249*, 1870–1901. [\[CrossRef\]](#)
28. Jana, N.R.; Gearheart, L.; Murphy, C.J. Evidence for seed-mediated nucleation in the chemical reduction of gold salts to gold nanoparticles. *Chem. Mater.* **2001**, *13*, 2313–2322. [\[CrossRef\]](#)
29. Nikoobakht, B.; El-Sayed, M.A. Preparation and growth mechanism of gold nanorods (NRs) using seed-mediated growth method. *Chem. Mater.* **2003**, *15*, 1957–1962. [\[CrossRef\]](#)
30. Yong, K.T.; Sahoo, Y.; Swihart, M.T.; Prasad, P.N. Synthesis and plasmonic properties of silver and gold nanoshells on polystyrene cores of different size and of gold–silver core–shell nanostructures. *Colloids Surf. A Physicochem. Eng. Asp.* **2006**, *290*, 89–105. [\[CrossRef\]](#)
31. Oldenburg, S.; Averitt, R.; Westcott, S.; Halas, N. Nanoengineering of optical resonances. *Chem. Phys. Lett.* **1998**, *288*, 243–247. [\[CrossRef\]](#)
32. Pham, T.; Jackson, J.B.; Halas, N.J.; Lee, T.R. Preparation and characterization of gold nanoshells coated with self-assembled monolayers. *Langmuir* **2002**, *18*, 4915–4920. [\[CrossRef\]](#)
33. Prodan, E.; Radloff, C.; Halas, N.J.; Nordlander, P. A hybridization model for the plasmon response of complex nanostructures. *Science* **2003**, *302*, 419–422. [\[CrossRef\]](#) [\[PubMed\]](#)
34. Skrabalak, S.E.; Chen, J.; Sun, Y.; Lu, X.; Au, L.; Copley, C.M.; Xia, Y. Gold nanocages: Synthesis, properties, and applications. *Acc. Chem. Res.* **2008**, *41*, 1587–1595. [\[CrossRef\]](#) [\[PubMed\]](#)

35. Elia, P.; Zach, R.; Hazan, S.; Kolusheva, S.; Porat, Z.e.; Zeiri, Y. Green synthesis of gold nanoparticles using plant extracts as reducing agents. *Int. J. Nanomed.* **2014**, *9*, 4007.
36. Yulizar, Y.; Utari, T.; Ariyanta, H.A.; Maulina, D. Green method for synthesis of gold nanoparticles using polyscias scutellaria leaf extract under uv light and their catalytic activity to reduce methylene blue. *J. Nanomater.* **2017**, *2017*, 3079636. [[CrossRef](#)]
37. ElMitwalli, O.S.; Barakat, O.A.; Daoud, R.M.; Akhtar, S.; Henari, F.Z. Green synthesis of gold nanoparticles using cinnamon bark extract, characterization, and fluorescence activity in Au/eosin Y assemblies. *J. Nanopart. Res.* **2020**, *22*, 309. [[CrossRef](#)]
38. Derjaguin, B.; Landau, L. The theory of stability of highly charged lyophobic sols and coalescence of highly charged particles in electrolyte solutions. *Acta Physicochim. URSS* **1941**, *14*, 58.
39. Marshall, C.E. Theory of the stability of lyophobic colloids. The interaction of particles having an electric double layer. E. J. W. Verwey and J. T. G. Overbeek, with the collaboration of K. van Ness. Elsevier, New York-Amsterdam. *J. Polym. Sci.* **1948**, *4*, 413–414. [[CrossRef](#)]
40. Goršak, T.; Makovec, D.; Javornik, U.; Belec, B.; Kralj, S.; Lisjak, D. A functionalization strategy for the dispersion of permanently magnetic barium-hexaferrite nanoplatelets in complex biological media. *Colloids Surf. A: Physicochem. Eng. Asp.* **2019**, *573*, 119–127. [[CrossRef](#)]
41. Laurent, S.; Forge, D.; Port, M.; Roch, A.; Robic, C.; Vander Elst, L.; Muller, R.N. Magnetic iron oxide nanoparticles: Synthesis, stabilization, vectorization, physicochemical characterizations, and biological applications. *Chem. Rev.* **2008**, *108*, 2064–2110. [[CrossRef](#)]
42. Heinz, H.; Pramanik, C.; Heinz, O.; Ding, Y.; Mishra, R.K.; Marchon, D.; Flatt, R.J.; Estrela-Lopis, I.; Llop, J.; Moya, S. Nanoparticle decoration with surfactants: Molecular interactions, assembly, and applications. *Surf. Sci. Rep.* **2017**, *72*, 1–58. [[CrossRef](#)]
43. Zhou, W.; Gao, X.; Liu, D.; Chen, X. Gold nanoparticles for in vitro diagnostics. *Chem. Rev.* **2015**, *115*, 10575–10636. [[CrossRef](#)] [[PubMed](#)]
44. Ramos, D.; Malvar, O.; Davis, Z.J.; Tamayo, J.; Calleja, M. Nanomechanical plasmon spectroscopy of single gold nanoparticles. *Nano Lett.* **2018**, *18*, 7165–7170. [[CrossRef](#)] [[PubMed](#)]
45. Tan, S.F.; Raj, S.; Bisht, G.; Annadata, H.V.; Nijhuis, C.A.; Král, P.; Mirsaidov, U. Nanoparticle interactions guided by shape-dependent hydrophobic forces. *Adv. Mater.* **2018**, *30*, 1707077. [[CrossRef](#)] [[PubMed](#)]
46. He, M.Q.; Chen, S.; Yao, K.; Meng, J.; Wang, K.; Yu, Y.L.; Wang, J.H. Precisely tuning LSPR property via “peptide-encoded” morphological evolution of gold nanorods for quantitative visualization of enzyme activity. *Anal. Chem.* **2019**, *92*, 1395–1401. [[CrossRef](#)]
47. Ogunyankin, M.O.; Shin, J.E.; Lapotko, D.O.; Ferry, V.E.; Zasadzinski, J.A. Optimizing the NIR fluence threshold for nanobubble generation by controlled synthesis of 10–40 nm hollow gold nanoshells. *Adv. Funct. Mater.* **2018**, *28*, 1705272. [[CrossRef](#)]
48. Bhalla, N.; Jain, A.; Lee, Y.; Shen, A.Q.; Lee, D. Dewetting metal nanofilms—Effect of substrate on refractive index sensitivity of nanoplasmonic gold. *Nanomaterials* **2019**, *9*, 1530. [[CrossRef](#)]
49. Luo, Z.; Zheng, K.; Xie, J. Engineering ultrasmall water-soluble gold and silver nanoclusters for biomedical applications. *Chem. Commun.* **2014**, *50*, 5143–5155. [[CrossRef](#)]
50. Zhang, L.; Wang, E. Metal nanoclusters: New fluorescent probes for sensors and bioimaging. *Nano Today* **2014**, *9*, 132–157. [[CrossRef](#)]
51. Doong, R.a.; Kim, H.; Sharma, V.K. *Interactions of Nanomaterials with Emerging Environmental Contaminants*; American Chemical Society: Washington, DC, USA, 2014. [[CrossRef](#)]
52. Zhou, C.; Yang, S.; Liu, J.; Yu, M.; Zheng, J. Luminescent gold nanoparticles: A new class of nanoprobe for biomedical imaging. *Exp. Biol. Med.* **2013**, *238*, 1199–1209. [[CrossRef](#)]
53. Barnes, W.L.; Dereux, A.; Ebbesen, T.W. Surface plasmon subwavelength optics. *Nature* **2003**, *424*, 824–830. [[CrossRef](#)]
54. Alivisatos, A.P. Semiconductor clusters, nanocrystals, and quantum dots. *Science* **1996**, *271*, 933–937. [[CrossRef](#)]
55. Kumar, A.; Das, N.; Satija, N.K.; Mandrah, K.; Roy, S.K.; Rayavarapu, R.G. A novel approach towards synthesis and characterization of non-cytotoxic gold nanoparticles using taurine as capping agent. *Nanomaterials* **2019**, *10*, 45. [[CrossRef](#)] [[PubMed](#)]
56. Gurunathan, S.; Han, J.; Park, J.H.; Kim, J.H. A green chemistry approach for synthesizing biocompatible gold nanoparticles. *Nanoscale Res. Lett.* **2014**, *9*, 248. [[CrossRef](#)]
57. Yang, Z.; Song, J.; Tang, W.; Fan, W.; Dai, Y.; Shen, Z.; Lin, L.; Cheng, S.; Liu, Y.; Niu, G. Stimuli-responsive nanotheranostics for real-time monitoring drug release by photoacoustic imaging. *Theranostics* **2019**, *9*, 526. [[CrossRef](#)]
58. Patil, M.P.; Kang, M.-j.; Niyonizigiye, I.; Singh, A.; Kim, J.-O.; Seo, Y.B.; Kim, G.-D. Extracellular synthesis of gold nanoparticles using the marine bacterium *Paracoccus haeundaensis* BC74171T and evaluation of their antioxidant activity and antiproliferative effect on normal and cancer cell lines. *Colloids Surf. B Biointerfaces* **2019**, *183*, 110455. [[CrossRef](#)] [[PubMed](#)]
59. Muthu, M.S.; Mei, L.; Feng, S.S. Nanotheranostics: Advanced nanomedicine for the integration of diagnosis and therapy. *Nanomedicine* **2014**, *9*, 1277–1280. [[CrossRef](#)]
60. Frank, D.; Tyagi, C.; Tomar, L.; Choonara, Y.E.; du Toit, L.C.; Kumar, P.; Penny, C.; Pillay, V. Overview of the role of nanotechnological innovations in the detection and treatment of solid tumors. *Int. J. Nanomed.* **2014**, *9*, 589.
61. Golombek, S.K.; May, J.N.; Theek, B.; Appold, L.; Drude, N.; Kiessling, F.; Lammers, T. Tumor targeting via EPR: Strategies to enhance patient responses. *Adv. Drug Deliv. Rev.* **2018**, *130*, 17–38. [[CrossRef](#)]
62. Vines, J.B.; Yoon, J.H.; Ryu, N.E.; Lim, D.J.; Park, H. Gold nanoparticles for photothermal cancer therapy. *Front. Chem.* **2019**, *7*, 167. [[CrossRef](#)] [[PubMed](#)]

63. Mantso, T.; Vasileiadis, S.; Anastopoulos, I.; Voulgaridou, G.-P.; Lampri, E.; Botaitis, S.; Kontomanolis, E.; Simopoulos, C.; Goussetis, G.; Franco, R. Hyperthermia induces therapeutic effectiveness and potentiates adjuvant therapy with non-targeted and targeted drugs in an in vitro model of human malignant melanoma. *Sci. Rep.* **2018**, *8*, 10724. [[CrossRef](#)] [[PubMed](#)]
64. Zhang, Y.; Zhan, X.; Xiong, J.; Peng, S.; Huang, W.; Joshi, R.; Cai, Y.; Liu, Y.; Li, R.; Yuan, K. Temperature-dependent cell death patterns induced by functionalized gold nanoparticle photothermal therapy in melanoma cells. *Sci. Rep.* **2018**, *8*, 8720. [[CrossRef](#)] [[PubMed](#)]
65. Guo, J.; Rahme, K.; He, Y.; Li, L.L.; Holmes, J.D.; O'Driscoll, C.M. Gold nanoparticles enlighten the future of cancer theranostics. *Int. J. Nanomed.* **2017**, *12*, 6131. [[CrossRef](#)] [[PubMed](#)]
66. Das, N.; Gopal, R.R. Impact of Isotropic and Anisotropic Plasmonic Metal Nanoparticles on Healthcare and Food Safety Management. In *Bio-Nano Interface*; Springer: Berlin/Heidelberg, Germany, 2022; pp. 1–20.
67. Kong, F.Y.; Zhang, J.W.; Li, R.F.; Wang, Z.X.; Wang, W.J.; Wang, W. Unique roles of gold nanoparticles in drug delivery, targeting and imaging applications. *Molecules* **2017**, *22*, 1445. [[CrossRef](#)] [[PubMed](#)]
68. Cobley, C.M.; Chen, J.; Cho, E.C.; Wang, L.V.; Xia, Y. Gold nanostructures: A class of multifunctional materials for biomedical applications. *Chem. Soc. Rev.* **2011**, *40*, 44–56. [[CrossRef](#)] [[PubMed](#)]
69. Zhou, B.; Yang, J.; Peng, C.; Zhu, J.; Tang, Y.; Zhu, X.; Shen, M.; Zhang, G.; Shi, X. PEGylated polyethylenimine-entrapped gold nanoparticles modified with folic acid for targeted tumor CT imaging. *Colloids Surf. B Biointerfaces* **2016**, *140*, 489–496. [[CrossRef](#)]
70. Yücel, O.; Şengelen, A.; Emik, S.; Önay-Uçar, E.; Arda, N.; Gürdağ, G. Folic acid-modified methotrexate-conjugated gold nanoparticles as nano-sized trojans for drug delivery to folate receptor-positive cancer cells. *Nanotechnology* **2020**, *31*, 355101. [[CrossRef](#)]
71. Zhang, J.; Li, C.; Zhang, X.; Huo, S.; Jin, S.; An, F.-F.; Wang, X.; Xue, X.; Okeke, C.; Duan, G. In vivo tumor-targeted dual-modal fluorescence/CT imaging using a nanoprobe co-loaded with an aggregation-induced emission dye and gold nanoparticles. *Biomaterials* **2015**, *42*, 103–111. [[CrossRef](#)]
72. Meir, R.; Shamalov, K.; Betzer, O.; Motiei, M.; Horovitz-Fried, M.; Yehuda, R.; Popovtzer, A.; Popovtzer, R.; Cohen, C.J. Nanomedicine for cancer immunotherapy: Tracking cancer-specific T-cells in vivo with gold nanoparticles and CT imaging. *ACS Nano* **2015**, *9*, 6363–6372. [[CrossRef](#)]
73. Wagner, D.S.; Delk, N.A.; Lukianova-Hleb, E.Y.; Hafner, J.H.; Farach-Carson, M.C.; Lapotko, D.O. The in vivo performance of plasmonic nanobubbles as cell theranostic agents in zebrafish hosting prostate cancer xenografts. *Biomaterials* **2010**, *31*, 7567–7574. [[CrossRef](#)]
74. Bao, C.; Conde, J.; Curtin, J.; Artzi, N.; Tian, F.; Cui, D. Bioresponsive antisense DNA gold nanobeacons as a hybrid in vivo theranostics platform for the inhibition of cancer cells and metastasis. *Sci. Rep.* **2015**, *5*, 12297. [[CrossRef](#)]
75. Conde, J.; Oliva, N.; Artzi, N. Implantable hydrogel embedded dark-gold nanoswitch as a theranostic probe to sense and overcome cancer multidrug resistance. *Proc. Natl. Acad. Sci. USA* **2015**, *112*, E1278–E1287. [[CrossRef](#)]
76. Conde, J.; Bao, C.; Tan, Y.; Cui, D.; Edelman, E.R.; Azevedo, H.S.; Byrne, H.J.; Artzi, N.; Tian, F. Dual targeted immunotherapy via in vivo delivery of biohybrid RNAi-peptide nanoparticles to tumor-associated macrophages and cancer cells. *Adv. Funct. Mater.* **2015**, *25*, 4183–4194. [[CrossRef](#)] [[PubMed](#)]
77. Deng, H.; Zhong, Y.; Du, M.; Liu, Q.; Fan, Z.; Dai, F.; Zhang, X. Theranostic self-assembly structure of gold nanoparticles for NIR photothermal therapy and X-Ray computed tomography imaging. *Theranostics* **2014**, *4*, 904. [[CrossRef](#)] [[PubMed](#)]
78. Meyers, J.D.; Cheng, Y.; Broome, A.M.; Agnes, R.S.; Schluchter, M.D.; Margevicius, S.; Wang, X.; Kenney, M.E.; Burda, C.; Basilion, J.P. Peptide-targeted gold nanoparticles for photodynamic therapy of brain cancer. *Part. Part. Syst. Charact.* **2015**, *32*, 448–457. [[CrossRef](#)] [[PubMed](#)]
79. Lukianova-Hleb, E.Y.; Ren, X.; Sawant, R.R.; Wu, X.; Torchilin, V.P.; Lapotko, D.O. On-demand intracellular amplification of chemoradiation with cancer-specific plasmonic nanobubbles. *Nat. Med.* **2014**, *20*, 778–784. [[CrossRef](#)] [[PubMed](#)]
80. Conde, J.; Bao, C.; Cui, D.; Baptista, P.V.; Tian, F. Antibody–drug gold nanoantennas with Raman spectroscopic fingerprints for in vivo tumour theranostics. *J. Control. Release* **2014**, *183*, 87–93. [[CrossRef](#)]
81. Shao, J.; Griffin, R.J.; Galanzha, E.I.; Kim, J.-W.; Koonce, N.; Webber, J.; Mustafa, T.; Biris, A.S.; Nedosekin, D.A.; Zharov, V.P. Photothermal nanodrugs: Potential of TNF-gold nanospheres for cancer theranostics. *Sci. Rep.* **2013**, *3*, 1293. [[CrossRef](#)] [[PubMed](#)]
82. Lu, W.; Zhang, G.; Zhang, R.; Flores, L.G.; Huang, Q.; Gelovani, J.G.; Li, C. Tumor site-specific silencing of NF-κB p65 by targeted hollow gold nanosphere-mediated photothermal transfection. *Cancer Res.* **2010**, *70*, 3177–3188. [[CrossRef](#)]
83. Chen, H.; Li, S.; Li, B.; Ren, X.; Li, S.; Mahounga, D.M.; Cui, S.; Gu, Y.; Achilefu, S. Folate-modified gold nanoclusters as near-infrared fluorescent probes for tumor imaging and therapy. *Nanoscale* **2012**, *4*, 6050–6064. [[CrossRef](#)]
84. Kim, S.-E.; Lee, B.-R.; Lee, H.; Jo, S.D.; Kim, H.; Won, Y.-Y.; Lee, J. Near-infrared plasmonic assemblies of gold nanoparticles with multimodal function for targeted cancer theragnosis. *Sci. Rep.* **2017**, *7*, 17327. [[CrossRef](#)]
85. You, J.; Zhang, R.; Xiong, C.; Zhong, M.; Melancon, M.; Gupta, S.; Nick, A.M.; Sood, A.K.; Li, C. Effective photothermal chemotherapy using doxorubicin-loaded gold nanospheres that target EphB4 receptors in tumors. *Cancer Res.* **2012**, *72*, 4777–4786. [[CrossRef](#)] [[PubMed](#)]
86. Kirui, D.K.; Khalidov, I.; Wang, Y.; Batt, C.A. Targeted near-IR hybrid magnetic nanoparticles for in vivo cancer therapy and imaging. *Nanomedicine* **2013**, *9*, 702–711. [[CrossRef](#)] [[PubMed](#)]
87. Zsigmondy, R.A.; Norton, J.F. *The Chemistry of Colloids*; John Wiley & Sons, Incorporated: Hoboken, NJ, USA, 1917.



88. Yang, C.Y.; Heinemann, K.; Yacaman, M.; Poppa, H. A structural analysis of small vapor-deposited “multiply twinned” gold particles. *Thin Solid Films* **1979**, *58*, 163–168. [[CrossRef](#)]
89. Renou, A.; Gillet, M. Growth of Au, Pt and Pd particles in a flowing argon system: Observations of decahedral and icosahedral structures. *Surf. Sci.* **1981**, *106*, 27–34. [[CrossRef](#)]
90. Wiesner, J.; Wokaun, A. Anisometric gold colloids. Preparation, characterization, and optical properties. *Chem. Phys. Lett.* **1989**, *157*, 569–575. [[CrossRef](#)]
91. Gans, R. Über die form ultramikroskopischer goldteilchen. *Ann. Phys.* **1912**, *342*, 881–900. [[CrossRef](#)]
92. Li, N.; Zhao, P.; Astruc, D. Anisotropic gold nanoparticles: Synthesis, properties, applications, and toxicity. *Angew. Chem. Int. Ed.* **2014**, *53*, 1756–1789. [[CrossRef](#)]
93. Lu, W.; Xiong, C.; Zhang, G.; Huang, Q.; Zhang, R.; Zhang, J.Z.; Li, C. Targeted photothermal ablation of murine melanomas with melanocyte-stimulating hormone analog-conjugated hollow gold nanospheres. *Clin. Cancer Res.* **2009**, *15*, 876–886. [[CrossRef](#)]
94. You, J.; Zhang, G.; Li, C. Exceptionally high payload of doxorubicin in hollow gold nanospheres for near-infrared light-triggered drug release. *ACS Nano* **2010**, *4*, 1033–1041. [[CrossRef](#)]
95. Wu, Y.-N.; Shieh, D.-B.; Yang, L.-X.; Sheu, H.-S.; Zheng, R.; Thordarson, P.; Chen, D.-H.; Braet, F. Characterization of iron core-gold shell nanoparticles for anti-cancer treatments: Chemical and structural transformations during storage and use. *Materials* **2018**, *11*, 2572. [[CrossRef](#)]
96. Loiseau, A.; Zhang, L.; Hu, D.; Salmain, M.; Mazouzi, Y.; Flack, R.; Liedberg, B.; Boujday, S. Core-shell gold/silver nanoparticles for localized surface Plasmon resonance-based naked-eye toxin biosensing. *ACS Appl. Mater. Interfaces* **2019**, *11*, 46462–46471. [[CrossRef](#)]
97. Ke, H.; Wang, J.; Tong, S.; Jin, Y.; Wang, S.; Qu, E.; Bao, G.; Dai, Z. Gold nanoshelled liquid perfluorocarbon magnetic nanocapsules: A nanotheranostic platform for bimodal ultrasound/magnetic resonance imaging guided photothermal tumor ablation. *Theranostics* **2014**, *4*, 12. [[CrossRef](#)] [[PubMed](#)]
98. Zhao, J.; Wallace, M.; Melancon, M.P. Cancer theranostics with gold nanoshells. *Nanomedicine* **2014**, *9*, 2041–2057. [[CrossRef](#)] [[PubMed](#)]
99. Huang, P.; Rong, P.; Lin, J.; Li, W.; Yan, X.; Zhang, M.G.; Nie, L.; Niu, G.; Lu, J.; Wang, W. Triphase interface synthesis of plasmonic gold bellflowers as near-infrared light mediated acoustic and thermal theranostics. *J. Am. Chem. Soc.* **2014**, *136*, 8307–8313. [[CrossRef](#)]
100. Bao, Z.; Liu, X.; Liu, Y.; Liu, H.; Zhao, K. Near-infrared light-responsive inorganic nanomaterials for photothermal therapy. *Asian J. Pharm. Sci.* **2016**, *11*, 349–364. [[CrossRef](#)]
101. Taruttis, A.; Lozano, N.; Nunes, A.; Jasim, D.A.; Beziere, N.; Herzog, E.; Kostarelos, K.; Ntziachristos, V. siRNA liposome-gold nanorod vectors for multispectral optoacoustic tomography theranostics. *Nanoscale* **2014**, *6*, 13451–13456. [[CrossRef](#)] [[PubMed](#)]
102. Zhang, M.; Kim, H.S.; Jin, T.; Moon, W.K. Near-infrared photothermal therapy using EGFR-targeted gold nanoparticles increases autophagic cell death in breast cancer. *J. Photochem. Photobiol. B Biol.* **2017**, *170*, 58–64. [[CrossRef](#)]
103. Hembury, M.; Chiappini, C.; Bertazzo, S.; Kalber, T.L.; Drisko, G.L.; Ogunlade, O.; Walker-Samuel, S.; Krishna, K.S.; Jumeaux, C.; Beard, P. Gold-silica quantum rattles for multimodal imaging and therapy. *Proc. Natl. Acad. Sci. USA* **2015**, *112*, 1959–1964. [[CrossRef](#)] [[PubMed](#)]
104. Ruan, S.; He, Q.; Gao, H. Matrix metalloproteinase triggered size-shrinkable gelatin-gold fabricated nanoparticles for tumor microenvironment sensitive penetration and diagnosis of glioma. *Nanoscale* **2015**, *7*, 9487–9496. [[CrossRef](#)]
105. Liu, Y.; Ashton, J.R.; Moding, E.J.; Yuan, H.; Register, J.K.; Fales, A.M.; Choi, J.; Whitley, M.J.; Zhao, X.; Qi, Y. A plasmonic gold nanostar theranostic probe for in vivo tumor imaging and photothermal therapy. *Theranostics* **2015**, *5*, 946. [[CrossRef](#)]
106. Zhong, J.; Wen, L.; Yang, S.; Xiang, L.; Chen, Q.; Xing, D. Imaging-guided high-efficient photoacoustic tumor therapy with targeting gold nanorods. *Nanomedicine* **2015**, *11*, 1499–1509. [[CrossRef](#)] [[PubMed](#)]
107. Yin, F.; Yang, C.; Wang, Q.; Zeng, S.; Hu, R.; Lin, G.; Tian, J.; Hu, S.; Lan, R.F.; Yoon, H.S. A light-driven therapy of pancreatic adenocarcinoma using gold nanorods-based nanocarriers for co-delivery of doxorubicin and siRNA. *Theranostics* **2015**, *5*, 818. [[CrossRef](#)] [[PubMed](#)]
108. Rahme, K.; Guo, J.; Holmes, J.D. Bioconjugated gold nanoparticles enhance siRNA delivery in prostate cancer cells. In *RNA Interference and Cancer Therapy*; Springer: Berlin/Heidelberg, Germany, 2019; pp. 291–301.
109. Hameed, M.; Panicker, S.; Abdallah, S.H.; Khan, A.A.; Han, C.; Chehimi, M.M.; Mohamed, A.A. Protein-coated aryl modified gold nanoparticles for cellular uptake study by osteosarcoma cancer cells. *Langmuir* **2020**, *36*, 11765–11775. [[CrossRef](#)] [[PubMed](#)]
110. Liu, J.; Ma, W.; Kou, W.; Shang, L.; Huang, R.; Zhao, J. Poly-amino acids coated gold nanorod and doxorubicin for synergistic photodynamic therapy and chemotherapy in ovarian cancer cells. *Biosci. Rep.* **2019**, *39*, BSR20192521. [[CrossRef](#)]
111. Chou, L.Y.; Chan, W.C. Fluorescence-tagged gold nanoparticles for rapidly characterizing the size-dependent biodistribution in tumor models. *Adv. Healthc. Mater.* **2012**, *1*, 714–721. [[CrossRef](#)]
112. Wang, G.; Li, Z.; Luo, X.; Yue, R.; Shen, Y.; Ma, N. DNA-templated nanoparticle complexes for photothermal imaging and labeling of cancer cells. *Nanoscale* **2018**, *10*, 16508–16520. [[CrossRef](#)]
113. Rayavarapu, R.G.; Petersen, W.; Ungureanu, C.; Post, J.N.; van Leeuwen, T.G.; Manohar, S. Synthesis and bioconjugation of gold nanoparticles as potential molecular probes for light-based imaging techniques. *Int. J. Biomed. Imaging* **2007**, *2007*, 10. [[CrossRef](#)]
114. Thanh, N.T.; Green, L.A. Functionalisation of nanoparticles for biomedical applications. *Nano Today* **2010**, *5*, 213–230. [[CrossRef](#)]

115. Cheng, W.; Dong, S.; Wang, E. Synthesis and self-assembly of cetyltrimethylammonium bromide-capped gold nanoparticles. *Langmuir* **2003**, *19*, 9434–9439. [\[CrossRef\]](#)
116. Chili, M.M.; Pullabhotla, V.R.; Revaprasadu, N. Synthesis of PVP capped gold nanoparticles by the UV-irradiation technique. *Mater. Lett.* **2011**, *65*, 2844–2847. [\[CrossRef\]](#)
117. Kurrey, R.; Deb, M.K.; Shrivastava, K.; Khalkho, B.R.; Nirmalkar, J.; Sinha, D.; Jha, S. Citrate-capped gold nanoparticles as a sensing probe for determination of cetyltrimethylammonium surfactant using FTIR spectroscopy and colorimetry. *Anal. Bioanal. Chem.* **2019**, *411*, 6943–6957. [\[CrossRef\]](#) [\[PubMed\]](#)
118. Das, N.; Kumar, A.; Rayavarapu, R.G. The role of deep eutectic solvents and carrageenan in synthesizing biocompatible anisotropic metal nanoparticles. *Beilstein J. Nanotechnol.* **2021**, *12*, 924–938. [\[CrossRef\]](#) [\[PubMed\]](#)
119. Wei, M.Z.; Deng, T.S.; Zhang, Q.; Cheng, Z.; Li, S. Seed-mediated synthesis of gold nanorods at low concentrations of CTAB. *ACS Omega* **2021**, *6*, 9188–9195. [\[CrossRef\]](#) [\[PubMed\]](#)
120. Fu, Q.; Ran, G.; Xu, W. Direct self-assembly of CTAB-capped Au nanotriangles. *Nano Res.* **2016**, *9*, 3247–3256. [\[CrossRef\]](#)
121. Verma, M.S.; Chen, P.Z.; Jones, L.; Gu, F.X. Branching and size of CTAB-coated gold nanostars control the colorimetric detection of bacteria. *RSC Adv.* **2014**, *4*, 10660–10668. [\[CrossRef\]](#)
122. Ngo, V.K.T.; Huynh, T.P.; Nguyen, D.G.; Nguyen, H.P.U.; Lam, Q.V.; Huynh, T.D. Synthesis and spectroscopic characterization of gold nanobipyramids prepared by a chemical reduction method. *Adv. Nat. Sci.: Nanosci. Nanotechnol.* **2015**, *6*, 045017. [\[CrossRef\]](#)
123. Lau, I.P.; Chen, H.; Wang, J.; Ong, H.C.; Leung, K.C.-F.; Ho, H.P.; Kong, S.K. In vitro effect of CTAB-and PEG-coated gold nanorods on the induction of eryptosis/erythroptosis in human erythrocytes. *Nanotoxicology* **2012**, *6*, 847–856. [\[CrossRef\]](#)
124. Duan, Q.; Yang, M.; Zhang, B.; Li, Y.; Zhang, Y.; Li, X.; Wang, J.; Zhang, W.; Sang, S. Gold nanoclusters modified mesoporous silica coated gold nanorods: Enhanced photothermal properties and fluorescence imaging. *J. Photochem. Photobiol. B Biol.* **2021**, *215*, 112111. [\[CrossRef\]](#)
125. Chakraborty, A.; Dave, H.; Mondal, B.; Nonappa; Khatun, E.; Pradeep, T. Shell-Isolated Assembly of Atomically Precise Nanoclusters on Gold Nanorods for Integrated Plasmonic-Luminescent Nanocomposites. *J. Phys. Chem. B* **2022**, *126*, 1842–1851. [\[CrossRef\]](#)
126. Chen, Y.; Xu, C.; Cheng, Y.; Cheng, Q. Photostability enhancement of silica-coated gold nanostars for photoacoustic imaging guided photothermal therapy. *Photoacoustics* **2021**, *23*, 100284. [\[CrossRef\]](#)
127. González-López, M.; Gutiérrez-Cárdenas, E.; Sánchez-Cruz, C.; Hernández-Paz, J.; Pérez, I.; Olivares-Trejo, J.; Hernández-González, O. Reducing the effective dose of cisplatin using gold nanoparticles as carriers. *Cancer Nano* **2020**, *11*, 4. [\[CrossRef\]](#)
128. Saeed, A.A.; Sánchez, J.L.A.; O’Sullivan, C.K.; Abbas, M.N. DNA biosensors based on gold nanoparticles-modified graphene oxide for the detection of breast cancer biomarkers for early diagnosis. *Bioelectrochemistry* **2017**, *118*, 91–99. [\[CrossRef\]](#) [\[PubMed\]](#)
129. Lee, C.S.; Kim, H.; Yu, J.; Yu, S.H.; Ban, S.; Oh, S.; Jeong, D.; Im, J.; Baek, M.J.; Kim, T.H. Doxorubicin-loaded oligonucleotide conjugated gold nanoparticles: A promising in vivo drug delivery system for colorectal cancer therapy. *Eur. J. Med. Chem.* **2017**, *142*, 416–423. [\[CrossRef\]](#) [\[PubMed\]](#)
130. Manivasagan, P.; Bharathiraja, S.; Bui, N.Q.; Jang, B.; Oh, Y.O.; Lim, I.G.; Oh, J. Doxorubicin-loaded fucoidan capped gold nanoparticles for drug delivery and photoacoustic imaging. *Int. J. Biol. Macromol.* **2016**, *91*, 578–588. [\[CrossRef\]](#)
131. Kalimuthu, K.; Lubin, B.-C.; Bazylevich, A.; Gellerman, G.; Shpilberg, O.; Luboshits, G.; Firer, M.A. Gold nanoparticles stabilize peptide-drug-conjugates for sustained targeted drug delivery to cancer cells. *J. Nanobiotechnol.* **2018**, *16*, 34. [\[CrossRef\]](#)
132. Sharma, A.; Tandon, A.; Tovey, J.C.; Gupta, R.; Robertson, J.D.; Fortune, J.A.; Klibanov, A.M.; Cowden, J.W.; Rieger, F.G.; Mohan, R.R. Polyethylenimine-conjugated gold nanoparticles: Gene transfer potential and low toxicity in the cornea. *Nanomedicine* **2011**, *7*, 505–513. [\[CrossRef\]](#)
133. Prades, R.; Guerrero, S.; Araya, E.; Molina, C.; Salas, E.; Zurita, E.; Selva, J.; Egea, G.; López-Iglesias, C.; Teixidó, M. Delivery of gold nanoparticles to the brain by conjugation with a peptide that recognizes the transferrin receptor. *Biomaterials* **2012**, *33*, 7194–7205. [\[CrossRef\]](#)
134. Sukhanova, A.; Bozrova, S.; Sokolov, P.; Berestovoy, M.; Karaulov, A.; Nabiev, I. Dependence of nanoparticle toxicity on their physical and chemical properties. *Nanoscale Res. Lett.* **2018**, *13*, 44. [\[CrossRef\]](#)
135. Das, N.; Kumar, A.; Kumar Roy, S.; Kumar Satija, N.; Raja Gopal, R. Bare plasmonic metal nanoparticles: Synthesis, characterisation and in vitro toxicity assessment on a liver carcinoma cell line. *IET Nanobiotechnol.* **2020**, *14*, 851–857. [\[CrossRef\]](#)
136. Moon, S.Y.; Kusunose, T.; Sekino, T. CTAB-assisted synthesis of size-and shape-controlled gold nanoparticles in SDS aqueous solution. *Mater. Lett.* **2009**, *63*, 2038–2040. [\[CrossRef\]](#)
137. Carnovale, C.; Bryant, G.; Shukla, R.; Bansal, V. Identifying trends in gold nanoparticle toxicity and uptake: Size, shape, capping ligand, and biological corona. *ACS Omega* **2019**, *4*, 242–256. [\[CrossRef\]](#)
138. Jia, Y.P.; Shi, K.; Liao, J.F.; Peng, J.R.; Hao, Y.; Qu, Y.; Chen, L.J.; Liu, L.; Yuan, X.; Qian, Z.Y. Effects of cetyltrimethylammonium bromide on the toxicity of gold nanorods both in vitro and in vivo: Molecular origin of cytotoxicity and inflammation. *Small Methods* **2020**, *4*, 1900799. [\[CrossRef\]](#)
139. Liu, K.; Zheng, Y.; Lu, X.; Thai, T.; Lee, N.A.; Bach, U.; Gooding, J.J. Biocompatible gold nanorods: One-step surface functionalization, highly colloidal stability, and low cytotoxicity. *Langmuir* **2015**, *31*, 4973–4980. [\[CrossRef\]](#) [\[PubMed\]](#)
140. Suk, J.S.; Xu, Q.; Kim, N.; Hanes, J.; Ensign, L.M. PEGylation as a strategy for improving nanoparticle-based drug and gene delivery. *Adv. Drug Deliv. Rev.* **2016**, *99*, 28–51. [\[CrossRef\]](#)



141. Chakraborty, S.; Joshi, P.; Shanker, V.; Ansari, Z.; Singh, S.P.; Chakrabarti, P. Contrasting effect of gold nanoparticles and nanorods with different surface modifications on the structure and activity of bovine serum albumin. *Langmuir* **2011**, *27*, 7722–7731. [\[CrossRef\]](#)
142. Egbuna, C.; Parmar, V.K.; Jeevanandam, J.; Ezzat, S.M.; Patrick-Iwuanyanwu, K.C.; Adetunji, C.O.; Khan, J.; Onyeike, E.N.; Uche, C.Z.; Akram, M. Toxicity of nanoparticles in biomedical application: Nanotoxicology. *J. Toxicol.* **2021**, *2021*, 9954443. [\[CrossRef\]](#)
143. Wan, J.; Wang, J.-H.; Liu, T.; Xie, Z.; Yu, X.-F.; Li, W. Surface chemistry but not aspect ratio mediates the biological toxicity of gold nanorods in vitro and in vivo. *Sci. Rep.* **2015**, *5*, 11398. [\[CrossRef\]](#)
144. Nazarenus, M.; Zhang, Q.; Soliman, M.G.; Del Pino, P.; Pelaz, B.; Carregal-Romero, S.; Rejman, J.; Rothen-Rutishauser, B.; Clift, M.J.; Zellner, R. In vitro interaction of colloidal nanoparticles with mammalian cells: What have we learned thus far? *Beilstein J. Nanotechnol.* **2014**, *5*, 1477–1490. [\[CrossRef\]](#)
145. Zhang, A.; Meng, K.; Liu, Y.; Pan, Y.; Qu, W.; Chen, D.; Xie, S. Absorption, distribution, metabolism, and excretion of nanocarriers in vivo and their influences. *Adv. Colloid Interface Sci.* **2020**, *284*, 102261. [\[CrossRef\]](#)
146. Mironava, T.; Hadjiargyrou, M.; Simon, M.; Jurukovski, V.; Rafailovich, M.H. Gold nanoparticles cellular toxicity and recovery: Effect of size, concentration and exposure time. *Nanotoxicology* **2010**, *4*, 120–137. [\[CrossRef\]](#)
147. Agrahari, K.; Rayavarapu, R.G. Chloride ions assisted synthesis of tunable gold nanorods: Seedless synthesis, characterization and in vitro toxicity studies. *Vacuum* **2019**, *166*, 377–384. [\[CrossRef\]](#)
148. Favi, P.M.; Gao, M.; Johana Sepúlveda Arango, L.; Ospina, S.P.; Morales, M.; Pavon, J.J.; Webster, T.J. Shape and surface effects on the cytotoxicity of gold nanoparticles: Gold nanospheres versus gold nanostars. *J. Biomed. Mater. Res. Part A* **2015**, *103*, 3449–3462. [\[CrossRef\]](#) [\[PubMed\]](#)
149. Sultana, S.; Djaker, N.; Boca-Farcu, S.; Salerno, M.; Charnaux, N.; Astilean, S.; Hlawaty, H.; de La Chapelle, M.L. Comparative toxicity evaluation of flower-shaped and spherical gold nanoparticles on human endothelial cells. *Nanotechnology* **2015**, *26*, 055101. [\[CrossRef\]](#) [\[PubMed\]](#)
150. Chu, Z.; Zhang, S.; Zhang, B.; Zhang, C.; Fang, C.-Y.; Rehor, I.; Cigler, P.; Chang, H.-C.; Lin, G.; Liu, R. Unambiguous observation of shape effects on cellular fate of nanoparticles. *Sci. Rep.* **2014**, *4*, 4495. [\[CrossRef\]](#)
151. Mateo, D.; Morales, P.; Ávalos, A.; Haza, A.I. Oxidative stress contributes to gold nanoparticle-induced cytotoxicity in human tumor cells. *Toxicol. Mech. Methods* **2014**, *24*, 161–172. [\[CrossRef\]](#)
152. Suvarna, S.; Das, U.; Kc, S.; Mishra, S.; Sudarshan, M.; Saha, K.D.; Dey, S.; Chakraborty, A.; Narayana, Y. Synthesis of a novel glucose capped gold nanoparticle as a better theranostic candidate. *PLoS ONE* **2017**, *12*, e0178202. [\[CrossRef\]](#)
153. Patungwasa, W.; Hodak, J.H. pH tunable morphology of the gold nanoparticles produced by citrate reduction. *Mater. Chem. Phys.* **2008**, *108*, 45–54. [\[CrossRef\]](#)
154. Lasagna-Reeves, C.; Gonzalez-Romero, D.; Barria, M.; Olmedo, I.; Clos, A.; Ramanujam, V.S.; Urayama, A.; Vergara, L.; Kogan, M.J.; Soto, C. Bioaccumulation and toxicity of gold nanoparticles after repeated administration in mice. *Biochem. Biophys. Res. Commun.* **2010**, *393*, 649–655. [\[CrossRef\]](#)
155. Maiorano, G.; Sabella, S.; Sorce, B.; Brunetti, V.; Malvindi, M.A.; Cingolani, R.; Pompa, P.P. Effects of cell culture media on the dynamic formation of protein–nanoparticle complexes and influence on the cellular response. *ACS Nano* **2010**, *4*, 7481–7491. [\[CrossRef\]](#)
156. Paino, I.M.M.; Marangoni, V.S.; de Oliveira, R.d.C.S.; Antunes, L.M.G.; Zucolotto, V. Cyto and genotoxicity of gold nanoparticles in human hepatocellular carcinoma and peripheral blood mononuclear cells. *Toxicol. Lett.* **2012**, *215*, 119–125. [\[CrossRef\]](#)
157. Sharma, S.; Bijwe, J.; Kumar, M. Comparison between nano- and micro-sized copper particles as fillers in NAO friction materials. *Nanomater. Nanotechnol.* **2013**, *3*, 12. [\[CrossRef\]](#)
158. Chatteraj, S.; Amin, M.A.; Mohapatra, S.; Ghosh, S.; Bhattacharyya, K. Cancer cell imaging using in situ generated gold nanoclusters. *ChemPhysChem* **2016**, *17*, 61–68. [\[CrossRef\]](#) [\[PubMed\]](#)
159. Pan, Y.; Neuss, S.; Leifert, A.; Fischler, M.; Wen, F.; Simon, U.; Schmid, G.; Brandau, W.; Jahnen-Dechent, W. Size-dependent cytotoxicity of gold nanoparticles. *Small* **2007**, *3*, 1941–1949. [\[CrossRef\]](#) [\[PubMed\]](#)
160. Zhang, C.; Zhou, Z.; Qian, Q.; Gao, G.; Li, C.; Feng, L.; Wang, Q.; Cui, D. Glutathione-capped fluorescent gold nanoclusters for dual-modal fluorescence/X-ray computed tomography imaging. *J. Mater. Chem. B* **2013**, *1*, 5045–5053. [\[CrossRef\]](#) [\[PubMed\]](#)
161. Zhu, X.M.; Fang, C.; Jia, H.; Huang, Y.; Cheng, C.H.; Ko, C.H.; Chen, Z.; Wang, J.; Wang, Y.-X.J. Cellular uptake behaviour, photothermal therapy performance, and cytotoxicity of gold nanorods with various coatings. *Nanoscale* **2014**, *6*, 11462–11472. [\[CrossRef\]](#)
162. Li, Y.; Wang, J.; Zhao, F.; Bai, B.; Nie, G.; Nel, A.E.; Zhao, Y. Nanomaterial libraries and model organisms for rapid high-content analysis of nanosafety. *Natl. Sci. Rev.* **2018**, *5*, 365–388. [\[CrossRef\]](#)
163. Bahamonde, J.; Brenseke, B.; Chan, M.Y.; Kent, R.D.; Vikesland, P.J.; Prater, M.R. Gold nanoparticle toxicity in mice and rats: Species differences. *Toxicol. Pathol.* **2018**, *46*, 431–443. [\[CrossRef\]](#)
164. Müller, B.; Grossniklaus, U. Model organisms—A historical perspective. *J. Proteom.* **2010**, *73*, 2054–2063. [\[CrossRef\]](#)
165. Zhang, X.-D.; Wu, D.; Shen, X.; Liu, P.-X.; Fan, F.-Y.; Fan, S.-J. In vivo renal clearance, biodistribution, toxicity of gold nanoclusters. *Biomaterials* **2012**, *33*, 4628–4638. [\[CrossRef\]](#)
166. Meng, J.; Ji, Y.; Liu, J.; Cheng, X.; Guo, H.; Zhang, W.; Wu, X.; Xu, H. Using gold nanorods core/silver shell nanostructures as model material to probe biodistribution and toxic effects of silver nanoparticles in mice. *Nanotoxicology* **2014**, *8*, 686–696. [\[CrossRef\]](#)

167. Bailly, A.L.; Correard, F.; Popov, A.; Tselikov, G.; Chaspoul, F.; Appay, R.; Al-Kattan, A.; Kabashin, A.V.; Braguer, D.; Esteve, M.-A. In vivo evaluation of safety, biodistribution and pharmacokinetics of laser-synthesized gold nanoparticles. *Sci. Rep.* **2019**, *9*, 12890. [[CrossRef](#)] [[PubMed](#)]
168. Sadauskas, E.; Wallin, H.; Stoltenberg, M.; Vogel, U.; Doering, P.; Larsen, A.; Danscher, G. Kupffer cells are central in the removal of nanoparticles from the organism. *Part. Fibre Toxicol.* **2007**, *4*, 10. [[CrossRef](#)] [[PubMed](#)]
169. Li, J.; Chen, C.; Xia, T. Understanding Nanomaterial–Liver Interactions to Facilitate the Development of Safer Nanoapplications. *Adv. Mater.* **2022**, *34*, 2106456. [[CrossRef](#)] [[PubMed](#)]
170. Lopez-Chaves, C.; Soto-Alvaredo, J.; Montes-Bayon, M.; Bettmer, J.; Llopis, J.; Sanchez-Gonzalez, C. Gold nanoparticles: Distribution, bioaccumulation and toxicity. In vitro and in vivo studies. *Nanomedicine* **2018**, *14*, 1–12. [[CrossRef](#)]
171. Schmid, G.; Kreyling, W.G.; Simon, U. Toxic effects and biodistribution of ultrasmall gold nanoparticles. *Arch. Toxicol.* **2017**, *91*, 3011–3037. [[CrossRef](#)]
172. Sokolova, V.; Mekky, G.; van der Meer, S.B.; Seeds, M.C.; Atala, A.J.; Epple, M. Transport of ultrasmall gold nanoparticles (2 nm) across the blood–brain barrier in a six-cell brain spheroid model. *Sci. Rep.* **2020**, *10*, 18033. [[CrossRef](#)]
173. Pompa, P.P.; Vecchio, G.; Galeone, A.; Brunetti, V.; Sabella, S.; Maiorano, G.; Falqui, A.; Berton, G.; Cingolani, R. In vivo toxicity assessment of gold nanoparticles in *Drosophila melanogaster*. *Nano Res.* **2011**, *4*, 405–413. [[CrossRef](#)]
174. Lindner, J.R.; Link, J. Molecular imaging in drug discovery and development. *Circ. Cardiovasc. Imaging* **2018**, *11*, e005355. [[CrossRef](#)]
175. Janib, S.M.; Moses, A.S.; MacKay, J.A. Imaging and drug delivery using theranostic nanoparticles. *Adv. Drug Deliv. Rev.* **2010**, *62*, 1052–1063. [[CrossRef](#)]
176. Hainfeld, J.; Slatkin, D.; Focella, T.; Smilowitz, H. Gold nanoparticles: A new X-ray contrast agent. *Br. J. Radiol.* **2006**, *79*, 248–253. [[CrossRef](#)]
177. Dreifuss, T.; Betzer, O.; Shilo, M.; Popovtzer, A.; Motiei, M.; Popovtzer, R. A challenge for theranostics: Is the optimal particle for therapy also optimal for diagnostics? *Nanoscale* **2015**, *7*, 15175–15184. [[CrossRef](#)] [[PubMed](#)]
178. Blasiak, B.; van Veggel, F.C.; Tomanek, B. Applications of nanoparticles for MRI cancer diagnosis and therapy. *J. Nanomater.* **2013**, *2013*, 12. [[CrossRef](#)]
179. Topete, A.; Alatorre-Meda, M.; Iglesias, P.; Villar-Alvarez, E.M.; Barbosa, S.; Costoya, J.A.; Taboada, P.; Mosquera, V. Fluorescent drug-loaded, polymeric-based, branched gold nanoshells for localized multimodal therapy and imaging of tumoral cells. *ACS Nano* **2014**, *8*, 2725–2738. [[CrossRef](#)] [[PubMed](#)]
180. Hossain, M.K.; Cho, H.-Y.; Kim, K.-J.; Choi, J.-W. In situ monitoring of doxorubicin release from biohybrid nanoparticles modified with antibody and cell-penetrating peptides in breast cancer cells using surface-enhanced Raman spectroscopy. *Biosens. Bioelectron.* **2015**, *71*, 300–305. [[CrossRef](#)]
181. Fan, M.; Han, Y.; Gao, S.; Yan, H.; Cao, L.; Li, Z.; Liang, X.J.; Zhang, J. Ultrasmall gold nanoparticles in cancer diagnosis and therapy. *Theranostics* **2020**, *10*, 4944. [[CrossRef](#)] [[PubMed](#)]
182. Kwon, K.C.; Jo, E.; Kwon, Y.W.; Lee, B.; Ryu, J.H.; Lee, E.J.; Kim, K.; Lee, J. Superparamagnetic gold nanoparticles synthesized on protein particle scaffolds for cancer theragnosis. *Adv. Mater.* **2017**, *29*, 1701146. [[CrossRef](#)]
183. Liu, J.; Yu, M.; Zhou, C.; Yang, S.; Ning, X.; Zheng, J. Passive tumor targeting of renal-clearable luminescent gold nanoparticles: Long tumor retention and fast normal tissue clearance. *J. Am. Chem. Soc.* **2013**, *135*, 4978–4981. [[CrossRef](#)]
184. Han, S.; Bouchard, R.; Sokolov, K.V. Molecular photoacoustic imaging with ultra-small gold nanoparticles. *Biomed. Opt. Express* **2019**, *10*, 3472–3483. [[CrossRef](#)]
185. Chen, F.; Goel, S.; Hernandez, R.; Graves, S.A.; Shi, S.; Nickles, R.J.; Cai, W. Dynamic positron emission tomography imaging of renal clearable gold nanoparticles. *Small* **2016**, *12*, 2775–2782. [[CrossRef](#)]
186. Nonappa, N. Luminescent gold nanoclusters for bioimaging applications. *Beilstein J. Nanotechnol.* **2020**, *11*, 533–546. [[CrossRef](#)]
187. Arifin, D.R.; Long, C.M.; Gilad, A.A.; Alric, C.; Roux, S.; Tillement, O.; Link, T.W.; Arepally, A.; Bulte, J.W. Trimodal gadolinium-gold microcapsules containing pancreatic islet cells restore normoglycemia in diabetic mice and can be tracked by using US, CT, and positive-contrast MR imaging. *Radiology* **2011**, *260*, 790–798. [[CrossRef](#)] [[PubMed](#)]
188. Wu, R.; Peng, H.; Zhu, J.-J.; Jiang, L.-P.; Liu, J. Attaching DNA to gold nanoparticles with a protein corona. *Front. Chem.* **2020**, *8*, 121. [[CrossRef](#)] [[PubMed](#)]
189. Egorova, E.A.; van Rij, M.M.; Sommerdijk, N.; Gooris, G.S.; Bouwstra, J.A.; Boyle, A.L.; Kros, A. One peptide for them all: Gold nanoparticles of different sizes are stabilized by a common peptide amphiphile. *ACS Nano* **2020**, *14*, 5874–5886. [[CrossRef](#)] [[PubMed](#)]
190. Oliveira, J.P.; Prado, A.R.; Keijok, W.J.; Antunes, P.W.P.; Yapuchura, E.R.; Guimarães, M.C.C. Impact of conjugation strategies for targeting of antibodies in gold nanoparticles for ultrasensitive detection of 17 $\beta$ -estradiol. *Sci. Rep.* **2019**, *9*, 13859. [[CrossRef](#)]
191. Herizchi, R.; Abbasi, E.; Milani, M.; Akbarzadeh, A. Current methods for synthesis of gold nanoparticles. *Artif. Cells Nanomed. Biotechnol.* **2016**, *44*, 596–602. [[CrossRef](#)]
192. Javed, R.; Zia, M.; Naz, S.; Aisida, S.O.; ul Ain, N.; Ao, Q. Role of capping agents in the application of nanoparticles in biomedicine and environmental remediation: Recent trends and future prospects. *J. Nanobiotechnol.* **2020**, *18*, 172. [[CrossRef](#)]
193. Singh, P.; Pandit, S.; Mokkapati, V.; Garg, A.; Ravikumar, V.; Mijakovic, I. Gold nanoparticles in diagnostics and therapeutics for human cancer. *Int. J. Mol. Sci.* **2018**, *19*, 1979. [[CrossRef](#)]

194. Dreaden, E.C.; Austin, L.A.; Mackey, M.A.; El-Sayed, M.A. Size matters: Gold nanoparticles in targeted cancer drug delivery. *Ther. Deliv.* **2012**, *3*, 457–478. [\[CrossRef\]](#)
195. Kobayashi, H.; Watanabe, R.; Choyke, P.L. Improving conventional enhanced permeability and retention (EPR) effects; What is the appropriate target? *Theranostics* **2014**, *4*, 81. [\[CrossRef\]](#)
196. Maeda, H. Macromolecular therapeutics in cancer treatment: The EPR effect and beyond. *J. Control. Release* **2012**, *164*, 138–144. [\[CrossRef\]](#)
197. Spivak, M.Y.; Bubnov, R.V.; Yemets, I.M.; Lazarenko, L.M.; Tymoshok, N.O.; Ulberg, Z.R. Development and testing of gold nanoparticles for drug delivery and treatment of heart failure: A theranostic potential for PPP cardiology. *Epma J.* **2013**, *4*, 20. [\[CrossRef\]](#) [\[PubMed\]](#)
198. Zhang, X.; Teodoro, J.G.; Nadeau, J.L. Intratumoral gold-doxorubicin is effective in treating melanoma in mice. *Nanomedicine* **2015**, *11*, 1365–1375. [\[CrossRef\]](#) [\[PubMed\]](#)
199. Olusanya, T.O.; Haj Ahmad, R.R.; Ibegbu, D.M.; Smith, J.R.; Elkordy, A.A. Liposomal drug delivery systems and anticancer drugs. *Molecules* **2018**, *23*, 907. [\[CrossRef\]](#) [\[PubMed\]](#)
200. Dhar, S.; Daniel, W.L.; Giljohann, D.A.; Mirkin, C.A.; Lippard, S.J. Polyvalent oligonucleotide gold nanoparticle conjugates as delivery vehicles for platinum (IV) warheads. *J. Am. Chem. Soc.* **2009**, *131*, 14652–14653. [\[CrossRef\]](#) [\[PubMed\]](#)
201. Shi, P.; Liu, Z.; Dong, K.; Ju, E.; Ren, J.; Du, Y.; Li, Z.; Qu, X. A Smart “Sense-Act-Treat” System: Combining a Ratiometric pH Sensor with a Near Infrared Therapeutic Gold Nanocage. *Adv. Mater.* **2014**, *26*, 6635–6641. [\[CrossRef\]](#)
202. Svenson, S.; Wolfgang, M.; Hwang, J.; Ryan, J.; Eliasof, S. Preclinical to clinical development of the novel camptothecin nanopharmaceutical CRLX101. *J. Control. Release* **2011**, *153*, 49–55. [\[CrossRef\]](#)
203. Zhang, Y.; Jiang, K.; Qing, D.; Huang, B.; Jiang, J.; Wang, S.; Yan, C. Accumulation of camptothecin and 10-hydroxycamptothecin and the transcriptional expression of camptothecin biosynthetic genes in *Camptotheca acuminata* cambial meristematic and dedifferentiated cells. *RSC Adv.* **2017**, *7*, 12185–12193. [\[CrossRef\]](#)
204. Bao, H.; Zhang, Q.; Xu, H.; Yan, Z. Effects of nanoparticle size on antitumor activity of 10-hydroxycamptothecin-conjugated gold nanoparticles: In vitro and in vivo studies. *Int. J. Nanomed.* **2016**, *11*, 929.
205. Ng, C.T.; Tang, F.M.A.; Li, J.J.e.; Ong, C.; Yung, L.L.Y.; Bay, B.H. Clathrin-mediated endocytosis of gold nanoparticles in vitro. *Nanomater. Plants Algae Microorg.* **2015**, *298*, 418–427.
206. Chanda, N.; Kattumuri, V.; Shukla, R.; Zambre, A.; Katti, K.; Upendran, A.; Kulkarni, R.R.; Kan, P.; Fent, G.M.; Casteel, S.W. Bombesin functionalized gold nanoparticles show in vitro and in vivo cancer receptor specificity. *Proc. Natl. Acad. Sci. USA* **2010**, *107*, 8760–8765. [\[CrossRef\]](#)
207. Ribeiro, R.S.G.; Belderbos, S.; Danhier, P.; Gallo, J.; Manshian, B.B.; Gallez, B.; Bañobre, M.; De Cuyper, M.; Soenen, S.J.; Gsell, W. Targeting tumor cells and neovascularization using RGD-functionalized magnetoliposomes. *Int. J. Nanomed.* **2019**, *14*, 5911. [\[CrossRef\]](#) [\[PubMed\]](#)
208. Choi, C.H.J.; Alabi, C.A.; Webster, P.; Davis, M.E. Mechanism of active targeting in solid tumors with transferrin-containing gold nanoparticles. *Proc. Natl. Acad. Sci. USA* **2010**, *107*, 1235–1240. [\[CrossRef\]](#) [\[PubMed\]](#)
209. Ahmed, M.; Pan, D.W.; Davis, M.E. Lack of in vivo antibody dependent cellular cytotoxicity with antibody containing gold nanoparticles. *Bioconjug. Chem.* **2015**, *26*, 812–816. [\[CrossRef\]](#) [\[PubMed\]](#)
210. Qian, Y.; Qiu, M.; Wu, Q.; Tian, Y.; Zhang, Y.; Gu, N.; Li, S.; Xu, L.; Yin, R. Enhanced cytotoxic activity of cetuximab in EGFR-positive lung cancer by conjugating with gold nanoparticles. *Sci. Rep.* **2014**, *4*, 1–8. [\[CrossRef\]](#) [\[PubMed\]](#)
211. Karmani, L.; Labar, D.; Valembois, V.; Bouchat, V.; Nagaswaran, P.G.; Bol, A.; Gillart, J.; Levêque, P.; Bouzin, C.; Bonifazi, D. Antibody-functionalized nanoparticles for imaging cancer: Influence of conjugation to gold nanoparticles on the biodistribution of <sup>89</sup>Zr-labeled cetuximab in mice. *Contrast Media Mol. Imaging* **2013**, *8*, 402–408. [\[CrossRef\]](#)
212. Kao, H.-W.; Lin, Y.-Y.; Chen, C.-C.; Chi, K.-H.; Tien, D.-C.; Hsia, C.-C.; Lin, W.-J.; Chen, F.-D.; Lin, M.-H.; Wang, H.-E. Biological characterization of cetuximab-conjugated gold nanoparticles in a tumor animal model. *Nanotechnology* **2014**, *25*, 295102. [\[CrossRef\]](#)
213. Van de Broek, B.; Devoogdt, N.; D'Hollander, A.; Gijs, H.-L.; Jans, K.; Lagae, L.; Muyldermans, S.; Maes, G.; Borghs, G. Specific cell targeting with nanobody conjugated branched gold nanoparticles for photothermal therapy. *ACS Nano* **2011**, *5*, 4319–4328. [\[CrossRef\]](#)
214. Fernández, M.; Javaid, F.; Chudasama, V. Advances in targeting the folate receptor in the treatment/imaging of cancers. *Chem. Sci.* **2018**, *9*, 790–810. [\[CrossRef\]](#)
215. Bahrami, B.; Mohammadnia-Afrouzi, M.; Bakhshaei, P.; Yazdani, Y.; Ghalamfarsa, G.; Yousefi, M.; Sadreddini, S.; Jadidi-Niaragh, F.; Hojjat-Farsangi, M. Folate-conjugated nanoparticles as a potent therapeutic approach in targeted cancer therapy. *Tumor Biol.* **2015**, *36*, 5727–5742. [\[CrossRef\]](#)
216. Zhu, J.; Fu, F.; Xiong, Z.; Shen, M.; Shi, X. Dendrimer-entrapped gold nanoparticles modified with RGD peptide and alpha-tocopheryl succinate enable targeted theranostics of cancer cells. *Colloids Surf. B: Biointerfaces* **2015**, *133*, 36–42. [\[CrossRef\]](#)
217. Reissmann, S. Cell penetration: Scope and limitations by the application of cell-penetrating peptides. *J. Pept. Sci.* **2014**, *20*, 760–784. [\[CrossRef\]](#) [\[PubMed\]](#)
218. Nativo, P.; Prior, I.A.; Brust, M. Uptake and intracellular fate of surface-modified gold nanoparticles. *ACS Nano* **2008**, *2*, 1639–1644. [\[CrossRef\]](#) [\[PubMed\]](#)
219. De la Fuente, J.M.; Berry, C.C. Tat peptide as an efficient molecule to translocate gold nanoparticles into the cell nucleus. *Bioconjug. Chem.* **2005**, *16*, 1176–1180. [\[CrossRef\]](#) [\[PubMed\]](#)



220. Juan, A.; Cimas, F.J.; Bravo, I.; Pandiella, A.; Ocaña, A.; Alonso-Moreno, C. Antibody conjugation of nanoparticles as therapeutics for breast cancer treatment. *Int. J. Mol. Sci.* **2020**, *21*, 6018. [\[CrossRef\]](#)
221. Samec, T.; Boulos, J.; Gilmore, S.; Hazelton, A.; Alexander-Bryant, A. Peptide-based delivery of therapeutics in cancer treatment. *Mater. Today Bio* **2022**, *14*, 100248. [\[CrossRef\]](#)
222. Yu, M.K.; Park, J.; Jon, S. Targeting strategies for multifunctional nanoparticles in cancer imaging and therapy. *Theranostics* **2012**, *2*, 3. [\[CrossRef\]](#)
223. Samadian, H.; Hosseini-Nami, S.; Kamrava, S.K.; Ghaznavi, H.; Shakeri-Zadeh, A. Folate-conjugated gold nanoparticle as a new nanoplatform for targeted cancer therapy. *J. Cancer Res. Clin. Oncol.* **2016**, *142*, 2217–2229. [\[CrossRef\]](#)
224. Benov, L. Photodynamic therapy: Current status and future directions. *Med. Princ. Pract.* **2015**, *24*, 14–28. [\[CrossRef\]](#)
225. Lim, C.K.; Heo, J.; Shin, S.; Jeong, K.; Seo, Y.H.; Jang, W.D.; Park, C.R.; Park, S.Y.; Kim, S.; Kwon, I.C. Nanophotosensitizers toward advanced photodynamic therapy of Cancer. *Cancer Lett.* **2013**, *334*, 176–187. [\[CrossRef\]](#)
226. Yu, J.; Hsu, C.H.; Huang, C.C.; Chang, P.Y. Development of therapeutic Au–methylene blue nanoparticles for targeted photodynamic therapy of cervical cancer cells. *ACS Appl. Mater. Interfaces* **2015**, *7*, 432–441. [\[CrossRef\]](#)
227. Chen, Q.; Chen, J.; Yang, Z.; Zhang, L.; Dong, Z.; Liu, Z. NIR-II light activated photodynamic therapy with protein-capped gold nanoclusters. *Nano Res.* **2018**, *11*, 5657–5669. [\[CrossRef\]](#)
228. Mfouo-Tynga, I.; Houreld, N.N.; Abrahamse, H. Evaluation of cell damage induced by irradiated Zinc-Phthalocyanine-gold dendrimeric nanoparticles in a breast cancer cell line. *Biomed. J.* **2018**, *41*, 254–264. [\[CrossRef\]](#) [\[PubMed\]](#)
229. Cabral, R.M.; Baptista, P.V. The chemistry and biology of gold nanoparticle-mediated photothermal therapy: Promises and challenges. *Nano Life* **2013**, *3*, 1330001. [\[CrossRef\]](#)
230. Liu, Y.; Xu, M.; Chen, Q.; Guan, G.; Hu, W.; Zhao, X.; Qiao, M.; Hu, H.; Liang, Y.; Zhu, H. Gold nanorods/mesoporous silica-based nanocomposite as theranostic agents for targeting near-infrared imaging and photothermal therapy induced with laser. *Int. J. Nanomed.* **2015**, *10*, 4747. [\[CrossRef\]](#)
231. Feng, B.; Xu, Z.; Zhou, F.; Yu, H.; Sun, Q.; Wang, D.; Tang, Z.; Yu, H.; Yin, Q.; Zhang, Z. Near infrared light-actuated gold nanorods with cisplatin–polypeptide wrapping for targeted therapy of triple negative breast cancer. *Nanoscale* **2015**, *7*, 14854–14864. [\[CrossRef\]](#)
232. Xu, W.; Qian, J.; Hou, G.; Wang, Y.; Wang, J.; Sun, T.; Ji, L.; Suo, A.; Yao, Y. A dual-targeted hyaluronic acid-gold nanorod platform with triple-stimuli responsiveness for photodynamic/photothermal therapy of breast cancer. *Acta Biomater.* **2019**, *83*, 400–413. [\[CrossRef\]](#)
233. Liu, L.; Xie, H.-J.; Mu, L.-M.; Liu, R.; Su, Z.-B.; Cui, Y.-N.; Xie, Y.; Lu, W.-L. Functional chlorin gold nanorods enable to treat breast cancer by photothermal/photodynamic therapy. *Int. J. Nanomed.* **2018**, *13*, 8119. [\[CrossRef\]](#)
234. Liu, J.; Liang, H.; Li, M.; Luo, Z.; Zhang, J.; Guo, X.; Cai, K. Tumor acidity activating multifunctional nanoplatform for NIR-mediated multiple enhanced photodynamic and photothermal tumor therapy. *Biomaterials* **2018**, *157*, 107–124. [\[CrossRef\]](#)
235. Bai, L.Y.; Yang, X.Q.; An, J.; Zhang, L.; Zhao, K.; Qin, M.Y.; Fang, B.Y.; Li, C.; Xuan, Y.; Zhang, X.S. Multifunctional magnetic-hollow gold nanospheres for bimodal cancer cell imaging and photothermal therapy. *Nanotechnology* **2015**, *26*, 315701. [\[CrossRef\]](#)
236. Hughes, J.P.; Rees, S.; Kalindjian, S.B.; Philpott, K.L. Principles of early drug discovery. *Br. J. Pharmacol.* **2011**, *162*, 1239–1249. [\[CrossRef\]](#)
237. Conde, J.; Dias, J.T.; Grazú, V.; Moros, M.; Baptista, P.V.; de la Fuente, J.M. Revisiting 30 years of biofunctionalization and surface chemistry of inorganic nanoparticles for nanomedicine. *Front. Chem.* **2014**, *2*, 48. [\[CrossRef\]](#) [\[PubMed\]](#)
238. Carthew, R.W.; Sontheimer, E.J. Origins and mechanisms of miRNAs and siRNAs. *Cell* **2009**, *136*, 642–655. [\[CrossRef\]](#) [\[PubMed\]](#)
239. Huang, X.; Hu, Q.; Braun, G.B.; Pallaoro, A.; Morales, D.P.; Zasadzinski, J.; Clegg, D.O.; Reich, N.O. Light-activated RNA interference in human embryonic stem cells. *Biomaterials* **2015**, *63*, 70–79. [\[CrossRef\]](#) [\[PubMed\]](#)
240. Chen, Z.; Zhang, L.; He, Y.; Shen, Y.; Li, Y. Enhanced shRNA Delivery and ABCG2 Silencing by Charge-Reversible Layered Nanocarriers. *Small* **2015**, *11*, 952–962. [\[CrossRef\]](#) [\[PubMed\]](#)
241. Bishop, C.J.; Tzeng, S.Y.; Green, J.J. Degradable polymer-coated gold nanoparticles for co-delivery of DNA and siRNA. *Acta Biomater.* **2015**, *11*, 393–403. [\[CrossRef\]](#)
242. Conde, J.; Rosa, J.; Jesús, M.; Baptista, P.V. Gold-nanobeacons for simultaneous gene specific silencing and intracellular tracking of the silencing events. *Biomaterials* **2013**, *34*, 2516–2523. [\[CrossRef\]](#) [\[PubMed\]](#)
243. Shen, J.; Kim, H.C.; Mu, C.; Gentile, E.; Mai, J.; Wolfram, J.; Ji, L.n.; Ferrari, M.; Mao, Z.w.; Shen, H. Multifunctional gold nanorods for siRNA gene silencing and photothermal therapy. *Adv. Healthc. Mater.* **2014**, *3*, 1629–1637. [\[CrossRef\]](#)
244. Bonoiu, A.C.; Bergey, E.J.; Ding, H.; Hu, R.; Kumar, R.; Yong, K.-T.; Prasad, P.N.; Mahajan, S.; Picchione, K.E.; Bhattacharjee, A. Gold nanorod–siRNA induces efficient in vivo gene silencing in the rat hippocampus. *Nanomedicine* **2011**, *6*, 617–630. [\[CrossRef\]](#)
245. Randeria, P.S.; Seeger, M.A.; Wang, X.-Q.; Wilson, H.; Shipp, D.; Mirkin, C.A.; Paller, A.S. siRNA-based spherical nucleic acids reverse impaired wound healing in diabetic mice by ganglioside GM3 synthase knockdown. *Proc. Natl. Acad. Sci. USA* **2015**, *112*, 5573–5578. [\[CrossRef\]](#)
246. Conde, J.; Ambrosone, A.; Sanz, V.; Hernandez, Y.; Marchesano, V.; Tian, F.; Child, H.; Berry, C.C.; Ibarra, M.R.; Baptista, P.V. Design of multifunctional gold nanoparticles for in vitro and in vivo gene silencing. *ACS Nano* **2012**, *6*, 8316–8324. [\[CrossRef\]](#)
247. Rosa, J.; Conde, J.; Jesus, M.; Lima, J.C.; Baptista, P.V. Gold-nanobeacons for real-time monitoring of RNA synthesis. *Biosens. Bioelectron.* **2012**, *36*, 161–167. [\[CrossRef\]](#) [\[PubMed\]](#)

248. Baptista, P.; Conde, J.; Rosa, J. Gold-Nanobeacons as a theranostic system for the detection and inhibition of specific genes. *Protoc. Exch.* **2013**. [CrossRef]
249. Conde, J.; De La Fuente, J.; Baptista, P. In vitro transcription and translation inhibition via DNA functionalized gold nanoparticles. *Nanotechnology* **2010**, *21*, 505101. [CrossRef] [PubMed]
250. Libutti, S.K.; Paciotti, G.F.; Byrnes, A.A.; Alexander, H.R.; Gannon, W.E.; Walker, M.; Seidel, G.D.; Yuldasheva, N.; Tamarkin, L. Phase I and pharmacokinetic studies of CYT-6091, a novel PEGylated colloidal gold-rhTNF nanomedicine. *Clin. Cancer Res.* **2010**, *16*, 6139–6149. [CrossRef]
251. Staves, B. Pilot Study of Aurolase™ Therapy in Refractory and/or Recurrent Tumors of the Head and Neck. ClinicalTrials.gov Identifier: NCT00848042; 2010. Available online: <https://clinicaltrials.gov/ct2/show/NCT00848042> (accessed on 1 November 2022).
252. Nanospectra Biosciences, Inc. *Efficacy Study of AuroLase Therapy in Subjects with Primary and/or Metastatic Lung Tumors*; ClinicalTrials.gov [Internet]; National Library of Medicine: Bethesda, MD, USA, 2000.
253. Kumthekar, P.; Rademaker, A.; Ko, C.; Dixit, K.; Schwartz, M.A.; Sonabend, A.M.; Sharp, L.; Lukas, R.V.; Stupp, R.; Horbinski, C. A phase 0 first-in-human study using NU-0129: A gold base spherical nucleic acid (SNA) nanoconjugate targeting BCL2L12 in recurrent glioblastoma patients. *J. Clin. Oncol.* **2019**, *37*, 3012. [CrossRef]
254. Amal, H.; Leja, M.; Funka, K.; Skapars, R.; Sivins, A.; Ancans, G.; Liepniece-Karele, I.; Kikuste, I.; Lasina, I.; Haick, H. Detection of precancerous gastric lesions and gastric cancer through exhaled breath. *Gut* **2016**, *65*, 400–407. [CrossRef]
255. Rastinehad, A.R.; Anastos, H.; Wajswol, E.; Winoker, J.S.; Sfakianos, J.P.; Doppalapudi, S.K.; Carrick, M.R.; Knauer, C.J.; Taouli, B.; Lewis, S.C. Gold nanoshell-localized photothermal ablation of prostate tumors in a clinical pilot device study. *Proc. Natl. Acad. Sci. USA* **2019**, *116*, 18590–18596. [CrossRef]
256. Daima, H.K.; Selvakannan, P.; Shukla, R.; Bhargava, S.K.; Bansal, V. Fine-tuning the antimicrobial profile of biocompatible gold nanoparticles by sequential surface functionalization using polyoxometalates and lysine. *PLoS ONE* **2013**, *8*, e79676. [CrossRef]
257. Shi, J.; Kantoff, P.W.; Wooster, R.; Farokhzad, O.C. Cancer nanomedicine: Progress, challenges and opportunities. *Nat. Rev. Cancer* **2017**, *17*, 20–37. [CrossRef]
258. Ruozzi, B.; Belletti, D.; Sharma, H.S.; Sharma, A.; Muresanu, D.F.; Mössler, H.; Forni, F.; Vandelli, M.A.; Tosi, G. PLGA nanoparticles loaded cerebrolysin: Studies on their preparation and investigation of the effect of storage and serum stability with reference to traumatic brain injury. *Mol. Neurobiol.* **2015**, *52*, 899–912. [CrossRef]
259. Ma, S.; Zhou, J.; Zhang, Y.; He, Y.; Jiang, Q.; Yue, D.; Xu, X.; Gu, Z. Highly stable fluorinated nanocarriers with iRGD for overcoming the stability dilemma and enhancing tumor penetration in an orthotopic breast cancer. *ACS Appl. Mater. Interfaces* **2016**, *8*, 28468–28479. [CrossRef] [PubMed]
260. Wang, Y.; Santos, A.; Evdokiou, A.; Losic, D. An overview of nanotoxicity and nanomedicine research: Principles, progress and implications for cancer therapy. *J. Mater. Chem. B* **2015**, *3*, 7153–7172. [CrossRef] [PubMed]
261. Coradeghini, R.; Gioria, S.; García, C.P.; Nativo, P.; Franchini, F.; Gilliland, D.; Ponti, J.; Rossi, F. Size-dependent toxicity and cell interaction mechanisms of gold nanoparticles on mouse fibroblasts. *Toxicol. Lett.* **2013**, *217*, 205–216. [CrossRef]
262. Ji, Z.; Wang, X.; Zhang, H.; Lin, S.; Meng, H.; Sun, B.; George, S.; Xia, T.; Nel, A.E.; Zink, J.I. Designed synthesis of CeO<sub>2</sub> nanorods and nanowires for studying toxicological effects of high aspect ratio nanomaterials. *ACS Nano* **2012**, *6*, 5366–5380. [CrossRef] [PubMed]
263. Goodman, C.M.; McCusker, C.D.; Yilmaz, T.; Rotello, V.M. Toxicity of gold nanoparticles functionalized with cationic and anionic side chains. *Bioconjug. Chem.* **2004**, *15*, 897–900. [CrossRef] [PubMed]
264. Arvizo, R.; Bhattacharya, R.; Mukherjee, P. Gold nanoparticles: Opportunities and challenges in nanomedicine. *Expert Opin. Drug Deliv.* **2010**, *7*, 753–763. [CrossRef] [PubMed]

**Disclaimer/Publisher’s Note:** The statements, opinions and data contained in all publications are solely those of the individual author(s) and contributor(s) and not of MDPI and/or the editor(s). MDPI and/or the editor(s) disclaim responsibility for any injury to people or property resulting from any ideas, methods, instructions or products referred to in the content.